



Extrapolation-Based Regionalized Re-evaluation of the Global Estuarine Surface Area

Goulven G. Laruelle¹ · Judith A. Rosentreter^{2,3,4} · Pierre Regnier¹

Received: 27 March 2024 / Revised: 31 October 2024 / Accepted: 8 November 2024
© The Author(s) 2024

Abstract

At the interface between the continental and oceanic domains, estuaries are essential components of the land–ocean aquatic continuum. These coastal ecosystems play a significant role in biogeochemical cycles, as they transform and export large amounts of terrigenous carbon and nutrients from rivers to marine waters. Because of this intense biogeochemical processing, they are significant ecosystems in terms of greenhouse gas exchange with the atmosphere. However, in spite of recent advances in remote sensing and the need for accurate estimates to calculate regional and global estuarine budgets, the global quantification of the estuarine spatial extent available for gas exchange has not been updated in over a decade and remains poorly constrained. This is due to the lack of a global extensive database, the diversity of estuaries, and the controversial definition of their boundaries. To address these challenges, a hybrid approach was developed that combines the surface areas of over 700 estuaries worldwide (extracted from the literature or calculated using geographical information systems) with a novel extrapolation method to provide type-specific regional estimates for 45 regions. The three estuarine types considered are ‘tidal systems and deltas’, ‘lagoons’, and ‘fjords’. The upscaling formula applied is determined and calibrated using data from several regions where an extensive survey of total estuarine surface areas was available. The new global estimate of $733,801 \pm 39,892 \text{ km}^2$ (mean $\pm 2 \sigma$) is 31% lower than the previous global assessment. It also provides quantitative uncertainty estimates for regional and global estuarine surface areas as well as a breakdown between tidal systems and deltas ($294,956 \pm 30,780 \text{ km}^2$), lagoons ($179,946 \pm 12,056 \text{ km}^2$), and fjords ($259,899 \pm 22,328 \text{ km}^2$). This decrease of the global estuarine surface area is related to the novel method used in this study and does not reflect a temporal trend.

Keywords Estuaries · Estuarine surface area · Estuarine typology · Tidal systems · Deltas · Lagoons · Fjords · Greenhouse gas exchange · Global biogeochemical budgets

Introduction

Estuaries can broadly be defined as aquatic transition systems at the interface between continents and oceans where freshwater mixes with marine water (Pritchard 1967; Elliott and McLusky 2002; Crossland et al. 2005; Schwartz 2005; Potter et al. 2010; Elliott et al., 2024). As such, they connect the terrestrial, riverine, marine, and atmospheric biogeochemical cycles, making these ecosystems a critical component of the Land–Ocean Aquatic Continuum (LOAC), and have thus been the centre of a growing interest in recent decades (Billen et al. 1991; Cole et al. 2007; Cai 2011; Regnier et al. 2013a, 2022; Bauer et al., 2013). Estuaries are dynamic biogeochemical ecosystems where both extensive primary production (Eyre 1998; Cloern et al. 2014; Mackenzie et al. 2012; Woodland et al. 2015) and heterotrophic respiration take place (Bauer et al. 2013; Najjar et al. 2018;

Communicated by Richard Fulford

✉ Goulven G. Laruelle
goulven.gildas.laruelle@ulb.be

- ¹ Department of Geoscience, Environment & Society (DGES)-BGEOSYS, Université Libre de Bruxelles, 1050 Brussels, Belgium
- ² Yale Institute for Biospheric Studies, Yale University, New Haven, USA
- ³ Yale School of the Environment, Yale University, New Haven, USA
- ⁴ Faculty of Science and Engineering, Southern Cross University, Lismore, Australia

Battin et al. 2023). The complex interplay between physical, biological, and chemical processes in estuaries (e.g. Regnier et al. 1998, 2013b; Vanderborgh et al. 2002; Volta et al. 2016a, 2016b) profoundly modifies the carbon and nutrient riverine loads before their export to the continental shelves and, ultimately, the open ocean (Gattuso et al. 1998; Mackenzie et al. 1998; Mantoura et al., 1991). For example, they exchange significant amounts of greenhouse gases (GHGs) such as CO₂, CH₄, and N₂O with the atmosphere (Borges 2005; Borges et al. 2005; Chen et al. 2013; Laruelle et al. 2013; Wells et al. 2018), and on longer time scales, they can sequester large amounts of nutrients and carbon in their sediment (Nixon et al., 1996, Laruelle 2009; Smith et al. 2015; Bianchi et al. 2020; Regnier et al. 2022). Therefore, estuaries play a significant role in global biogeochemical cycles, as recognized in the latest global GHG budgets initiated by the Global Carbon Project (Friedlingstein et al. 2022; Tian et al. 2020; Saunio et al. 2020). Estuaries also host essential economical resources (Berbier et al., 2011) and a unique biodiversity (Kennish 2002; Leal Filho et al. 2022) and provide opportunities for coastal development. For instance, 14 out of 20 of the largest cities in the world are located near the mouth of a river and the worldwide economic worth of aquaculture production in 2018 (including aquatic plants and inland water production) was estimated at 263 billion USD (Bartley 2022), a large fraction of which is farmed in estuaries. Despite this strategic economic and scientific relevance, currently available estimates for global estuarine surface area remain poorly constrained, regionalized at a coarse spatial resolution, and have not been updated in over a decade (Dürr et al. 2011). Such lack of update may be surprising considering the recent improvement of remote sensing imagery and Geographic Information Systems (GIS), which in recent years have helped better constrain the spatial distribution of other coastal ecosystems such as mangrove forests (Bunting et al. 2022), tidal marshes (Tootchi et al. 2019), and intertidal mud flats (Murray et al. 2018). This knowledge gap translates into an incompressible source of uncertainty in global biogeochemical estuarine budgets, effectively hampering upscaling efforts.

The first published estimate of the global estuarine surface area dates back to 1973, when Woodwell et al. (1973) extrapolated a ratio of estuarine surface area per length of coastline (the ‘Woodwell ratio’) from a USA-based survey to the entire global coastline. For several decades, the resulting global estimate of 1.4×10^6 km² was the only available figure and was thus widely used to extrapolate GHG emissions from estuaries from local to global scales (Abril and Borges 2004; Borges 2005; Borges et al. 2005; Chen and Borges 2009; Frankignoulle et al., 1998; Jiang et al., 2008; Seitzinger and Kroeze, 1998). The same surface area estimate was also used to constrain the size of the estuarine compartment of several global box models (Mackenzie

et al. 1993, 1998, 2012; Ver 1998; Ver et al. 1999; Rabouille et al. 2001; Laruelle et al. 2009a, b) which have been used to investigate a range of issues including coastal anoxia, estuarine nutrient retention, GHG exchange between aquatic compartment and the atmosphere or the fate of carbon along its journey through the LOAC. Only in 2011 was this estimate revised by Dürr et al. (2011) using an approach similar to that of Woodwell et al. (1973) but refined by the use of type-specific ratios of estuarine surface area per length of coastline, which brought the estimate down to 1.067×10^6 km². This new value resulted in a downward revision of the global CO₂ emissions estimate from estuaries in the following years (Laruelle et al. 2010, 2013, Cai 2011, Borges and Abril, 2012; Chen et al. 2013). In addition to a global surface area reduction, this new estimate paved the way for a refined global analysis of the estuarine biogeochemical dynamics, since the type-specific assessment segregated fjords, tidal estuaries, small deltas, and lagoons, which typically exhibit distinct biogeochemical behaviours because of, for example, characteristic freshwater residence times spanning several orders of magnitude between estuary types (Dürr et al. 2011). Although a significant improvement since Woodwell et al. (1973), the updated surface area remained poorly constrained because the so-called ‘Woodwell ratios’ were only calibrated on very limited sections of the world (USA, Engle et al. 2007; UK, DEFRA, 2008; Australia, Digby et al. 1998; and Sweden, SMHI, 2009), and these national databases already highlighted significant inter-regional spatial variability which could not be accounted for. Furthermore, the spatial resolution of the estuarine typology (0.5°) used by Dürr et al. (2011) to calculate the lengths of coastlines implicitly assumed that only one type of estuary can be found within stretches of several tens of kilometres. Addressing these two drawbacks would require the use of ratios or extrapolation methods that could be calibrated for each region and each type using data from the region of interest. The work of Dürr et al. (2011) nonetheless sparked a significant interest from the scientific community not limited to the revision of GHG emissions from estuaries (Laruelle et al. 2010, 2013; Borges and Abril, 2012, Cai 2011; Chen et al. 2013; Bauer et al. 2013; Regnier et al. 2013a, 2022; Ciais et al., 2022). Indeed, the type-dependent residence times also calculated by Dürr et al. (2011) provided a reference for the first spatially explicit global estuarine modelling studies (Maavara et al., 2019; Laruelle 2009), which were previously limited to local or regional assessments in well-surveyed regions (Regnier et al. 2013b; Laruelle et al. 2017, 2019; Volta et al. 2016a).

In an age where remote sensing and GIS capabilities are sharply expanding, high-resolution global databases derived from satellite imagery are regularly updated for many types of ecosystems (e.g. Allen and Pavelsky 2018; Santoro et al. 2021; Reinhert et al., 2022). However,

several technical challenges including the complex definition of estuaries (Bianchi 2013; Dürr et al. 2011; Elliott and McLusky, 2002), the delineation of their boundaries (Pritchard 1967, Savenije, 2012), and their temporal variations (Jung et al., 2021) are still major hurdles to release such data product for estuarine surface areas at regional and global scales. While a growing number of national and regional estuarine databases have been published since the early 2000s (Alder 2003; CDELM, 2003), the vast majority of the global coastline remains scarcely monitored. In addition, the determination of estuarine surface areas by algorithms able to extract geometric properties from satellite imagery (Jung et al. 2021), although promising, is still far from an automated procedure able to identify each estuary over a continuous large stretch of coast. This technical challenge, in conjunction with an estimated global number of estuaries in the tens of thousands (Mc Sweeney et al., 2017), highlights the difficulty of reaching a global assessment in the foreseeable future despite a growing number of exhaustive regional censuses.

In this study, we use a hybrid method relying on GIS-derived calculations for a limited number of individual systems combined with an extrapolation strategy to provide regionalized estimates of estuarine surface areas distinguishing three estuarine types in 45 regions worldwide. Within each of these so-called MARCATS regions (for MARgins and CATchments Segmentation, Laruelle et al. 2013), we identify the ten largest estuarine systems for each estuary type and rank them by decreasing surface area before performing an extrapolation which allows estimating the total estuarine surface area of each region. This approach addresses the two limitations identified in the approach of Dürr et al. (2011) in the sense that the coefficients of the formula used for our extrapolation are fitted to the cumulative surface area derived from the 10 largest systems of the region, thus independently accounting for the geomorphological specificities of each region. We also provide the first quantitative estimate of the uncertainty over the calculated regional estuarine surface areas, which is essential for an accurate assessment of estuarine GHG budgets (Regnier et al. 2022). In this context, we also provide estuary-type specific surface area estimates for each of the RECCAP 2 regions (for the second Regional Carbon Cycle Assessment and Processes) as described in Ciais et al. (2022). Our revised surface area estimate and associated uncertainty have recently been used in a new observation-based meta-analysis of estuarine GHG budgets, including CO₂, CH₄, and N₂O (Rosentreter et al., 2023), highlighting that our revision has profound implications for our understanding of the role of estuaries in global carbon and nitrogen cycles.

Methods

Estuarine Definition and Typology

An estuary can be described as a coastal water body where marine and fresh waters mix above ground (Bianchi 2013; Schwatz, 2005; Pritchard 1967; Dürr et al. 2011). As such, they are characterized by numerous chemical (e.g. salinity, nutrients) and physical (e.g. tidal amplitude and energy) gradients and can widely vary in size and shape depending on their geological settings. A broad definition of the term ‘estuary’ includes systems as diverse as fjords, tidal embayments, deltas, alluvial estuaries, or lagoons. There is no consensus in the literature regarding the exact definitions of upstream and downstream boundaries of estuaries, and different limits may be used by different authors. Following Dürr et al. (2011), we use a geographical-based definition of the lower boundary at the interface with the coastal ocean corresponding to a virtual extension of the coastline regardless of the potential low salinity extension of estuarine waters onto the continental shelf (McKee et al. 2004). Not only can the global surface area of these so-called ‘riverine plumes’ amount to several million km² (Kang et al. 2013) but their spatial extent also varies over time with changing freshwater discharge, tidal amplitude, and wind-induced mixing. Our lower boundary for estuaries is consistent with the coastal baseline definition used by the United Nations Convention on the Law of the Sea (UNCLOS) or the concept of the bay closing line which only relies on the geographical extension of the coastline, thus excluding river plumes. Upstream, several criteria also exist to define the limit between estuarine and inland waters. The two most commonly used are the limits of the salinity intrusion and the length of the tidal influence (Bianchi 2013; Pritchard 1967), which can extend several times further inland (Dürr et al. 2011; Savenije et al., 2012). The tidal river, the area with almost no salinity (<0.5) but still under tidal influence, has a length that can be significant, up to several times the length of the salt intrusion (Savenije 2005), but its width is usually much narrower than in the brackish region of the estuary thus minimizing its contribution to the total surface area of the estuarine system. Moreover, many rivers are dammed before the natural end of the tidal influence or even the salinity intrusion, in which case the dam itself becomes the upstream limit of an estuary (e.g. Seine river, Laruelle et al. 2019). In this work, following Dürr et al. (2011), we exclude the tidal river as part of the estuary. Although we acknowledge that the intensity of some biogeochemical processes may be particularly high in this portion of the estuary, our choice is also motivated by the fact that, in a context of providing surface area estimates to constrain

biogeochemical budgets, the salinity limit is commonly used in such exercises as the frontier between estuarine and riverine domains (Seitzinger et al. 2005; Mayorga et al. 2010; Canadell et al., 2012). Furthermore, only the saline portion of estuaries displays markedly different physical and biogeochemical behaviours compared to that of rivers (Regnier et al. 2013b).

Inspired by the typology proposed by Dürr et al. (2011), we distinguish three major estuarine groups:

- 1) ‘Tidal systems and deltas’ which includes all open tidal systems from alluvial estuaries to tidal bays and rias (which are riverine valleys flooded by sea level rise) as well as deltas of any size, thus combining types I, II, and V of Dürr et al. (2011)’s typology
- 2) ‘Lagoons’, which include enclosed shallow estuarine systems with minimal tidal influence and relatively long water residence times, corresponding to types III in the Dürr et al. (2011) typology
- 3) ‘Fjords’, which include all fjords with typical U-shaped valleys created by glaciers as well as other coastal glacial depressions such as fjärds, defined as type IV in Dürr et al. (2011).

The original typology proposed by Dürr and colleagues thus relied on a larger number of classes than in our study. Here, we decided to merge small deltas (type I) and tidal systems (type II), because their distinction sometimes proved difficult to establish as many deltas (even the smaller ones) are often under the tidal influence (e.g. Mekong, Amazon, Ganges) while several stable tidal estuaries display multiple channels and branches (e.g. Pearl River estuary), a key feature of deltaic systems. Furthermore, Dürr et al. (2011) defined estuaries fed by very large rivers (Ericson et al., 2005) as a separate type devoid of internal filters, arguing that characteristic residence times of freshwater within the estuarine limits of such systems are very short and do not allow for significant biogeochemical processing of riverine material prior to its export onto the continental shelf. While this assertion is partly supported by observations (McKee et al. 2004), such consideration is not relevant to our analysis that solely focusses on the determination of surface areas. Moreover, in many estuarine systems, the seasonal variation in riverine discharge leads to residence times that may vary significantly throughout the year (Dai and Trenberth 2002; Du and Shen, 2016; Wei et al. 2022). Therefore, we merge types I, II, and V of Dürr et al. (2011)’s classification into a single class in our calculations.

Novel Upscaling Procedure

An autonomous algorithm able to systematically determine estuarine areas over a continuous stretch of coastline has

not yet been developed. In addition, performing such a task manually by individually determining the limits of each system through GIS would be a daunting task and has only been implemented at the regional scale in rare extensively surveyed zones (Engle et al. 2007; Digby et al. 1998). As a substitute for estuarine surface areas derived from an elusive global database, we developed an empirical prediction method that allows extrapolating the total surface area of a region from a limited number of measured systems. Somewhat similar approaches have been developed using scaling laws for the surface area and density of lakes (Downing et al. 2006) and other water bodies (Sagar 2007; Bhang et al. 2019). Using data extracted from several national databases with exhaustive coverage of estuaries (USA, Australia, New Zealand: Hume et al. 2016; South Korea: Jung et al. 2021; South Africa: Van Niekerk, et al. 2013), we tried to fit the cumulative surface area of estuaries ranked in decreasing order of size over a stretch of coast consistently against the number of estuaries within that stretch of coast with several formulas. The best fits across the different datasets were consistently obtained by an equation of the form:

$$S = \frac{a \times N}{b + N} \quad (1)$$

with S being the cumulative estuarine surface area (km^2), N the number of estuaries, and a (km^2) and b (unitless) the calibration coefficients. This equation, which plot is characterized by an initial steep increase converging toward a plateau implies that, as N tends toward infinity, S tends toward a , which thus corresponds to the asymptotic total surface area of the region (km^2). This function was retained for its limited number of input and fitting parameters. Preliminary tests performed by applying this approach on regions of varying sizes revealed that to be a robust predictor, the equation requires an exhaustive coverage of a stretch of coast long enough to ensure the inclusion of at least 30 systems, generally corresponding to several hundreds of kilometres. In order to take advantage of the apparent generic nature of Eq. (1), our extrapolation strategy consisted of first identifying and characterizing the ten largest estuaries of a given region and then fitting Eq. (1) on the basis of this limited dataset to calculate the theoretical total surface area of the region (calibration term a of Eq. 1). In order to comply with the constraints of the method regarding the size and number of estuaries within a stretch of coastline and to work with regions characterized by relatively homogeneous estuarine settings, we used the global MARCATS segmentation (Laruelle et al. 2013), which delineates the global coastline into 45 regions.

Within each MARCATS and for each estuary type, the determination of the surface areas of the 10 largest systems of each estuarine type was achieved through the inspection of national databases (Australia, New Zealand, Mexico, USA,

South Africa, South Korea, etc.), regional surveys (FAO, UNESCO), global databases (Sea Around Us, 2003), or published studies dedicated to a single or several systems. When no information was available from this literature search (24% of the systems), the surface areas were calculated individually using GIS. These calculations were performed in QGIS using the novel 30-m resolution global shoreline vector dataset (Sayre et al. 2018). Overall, a total of 735 individual estuary surface areas were gathered or calculated, 247 were extracted from various databases, 211 from the literature, and 277 were calculated. Those data were then sorted and fitted using Eq. (1) to derive the regionalized estuarine surface area for each MARCATS and each estuarine type. A schematic representation of the step-by-step procedure used to apply our novel approach to each MARCATS region is provided in Fig. 1. One interest of this regionalized approach is to capture the specificities of a region through the fit of the formula using regional data (i.e. the cumulative surface area of the largest estuaries of the region) as opposed to previous approaches that performed regional calculations using globally averaged parameters (Dürr et al. (2011) or Woodwell et al. (1973)). All calculations in this study were performed in MATLAB using the function *nlinfit* to determine the coefficients *a* and *b* in Eq. (1).

The goodness of fit of the model was evaluated using the mean squared error (MSE) calculated by the function *nlinfit* using the formula:

$$MSE = \frac{\sum R^2}{N - p} \tag{2}$$

where *R* is the residuals representing the mismatch between the observed and calculated values of *S* (i.e. the difference between the cumulative estuarine surface areas calculated using observed values and those predicted by the fitted Eq. 1 for each value of *N*), *N* is the number of systems for which a comparison can be performed between the model and the observations (i.e. 10 whenever possible), and *p* is the number of parameters of the fitting formula used (i.e. 2). The square root of this MSE was then reported to the average cumulated surface area of the dataset to provide a relative root mean square error (RRMSE) expressed as a percentage representing the relative deviation of the fitted model reported to the observations used to perform the extrapolation (10 for most MARCATS regions).

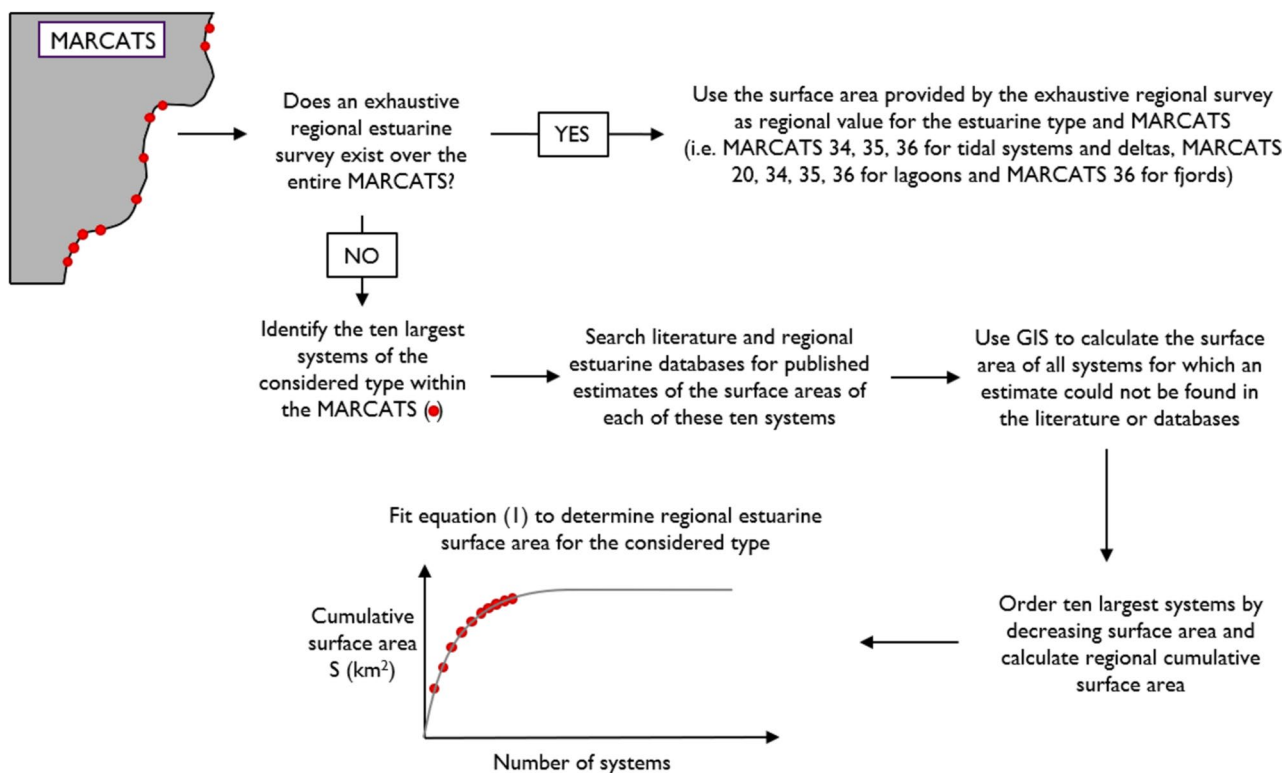


Fig. 1 Schematic representation of the step-by-step procedure used to calculate the type-specific estuarine surface area for each MARCATS region

Strategies to Quantitatively Constrain Uncertainties

Two different sources of uncertainties were accounted for in our calculations. The first, Δ_M , represents the uncertainty associated with our interpolation method, while the second, Δ_S , corresponds to the propagation at the regional scale of the uncertainty related to the determination of the surface area of individual systems δ_{Si} . Both Δ_M and Δ_S are expressed in square kilometres and can be summed quadratically (i.e. by calculating the square root of the sum of both terms squared) to quantify the total uncertainty Δ_T and are described in detail in the following.

In order to quantify the uncertainty attributed to the extrapolation method itself (Δ_M), the term δ_M , which represents the relative uncertainty (in %) associated with our extrapolation method had to be evaluated. To this end, our predictive equation was applied using the 5, 8, or 10 largest systems located in the few MARCATS for

which all estuaries (and thus the total regional surface area) were known and for which at least 30 estuaries of a given type were identified within the MARCATS. Five regions matched the above criteria for deltas and tidal systems: along the Pacific US coast (MARCATS 2) and along the Atlantic US coast (MARCATS 10), as well as along MARCATS 34, 35 (Australia), and 36 (New Zealand). Four had sufficient data coverage for lagoons: along MARCATS 20 (Mediterranean Sea), 34, 35 (Australia), and 36 (New Zealand). Unfortunately, no region matched our criteria for fjords as New Zealand is the only region containing fjords for which an exhaustive survey exists but the number of these systems is limited (11) and thus was not large enough to train our fitting algorithm. Based on this analysis, we found that the normalized standard deviations around the actual regional surface areas were 26, 12, and 9% for extrapolations relying on the 5, 8, and 10 largest systems, respectively (Fig. 2). These percentages were

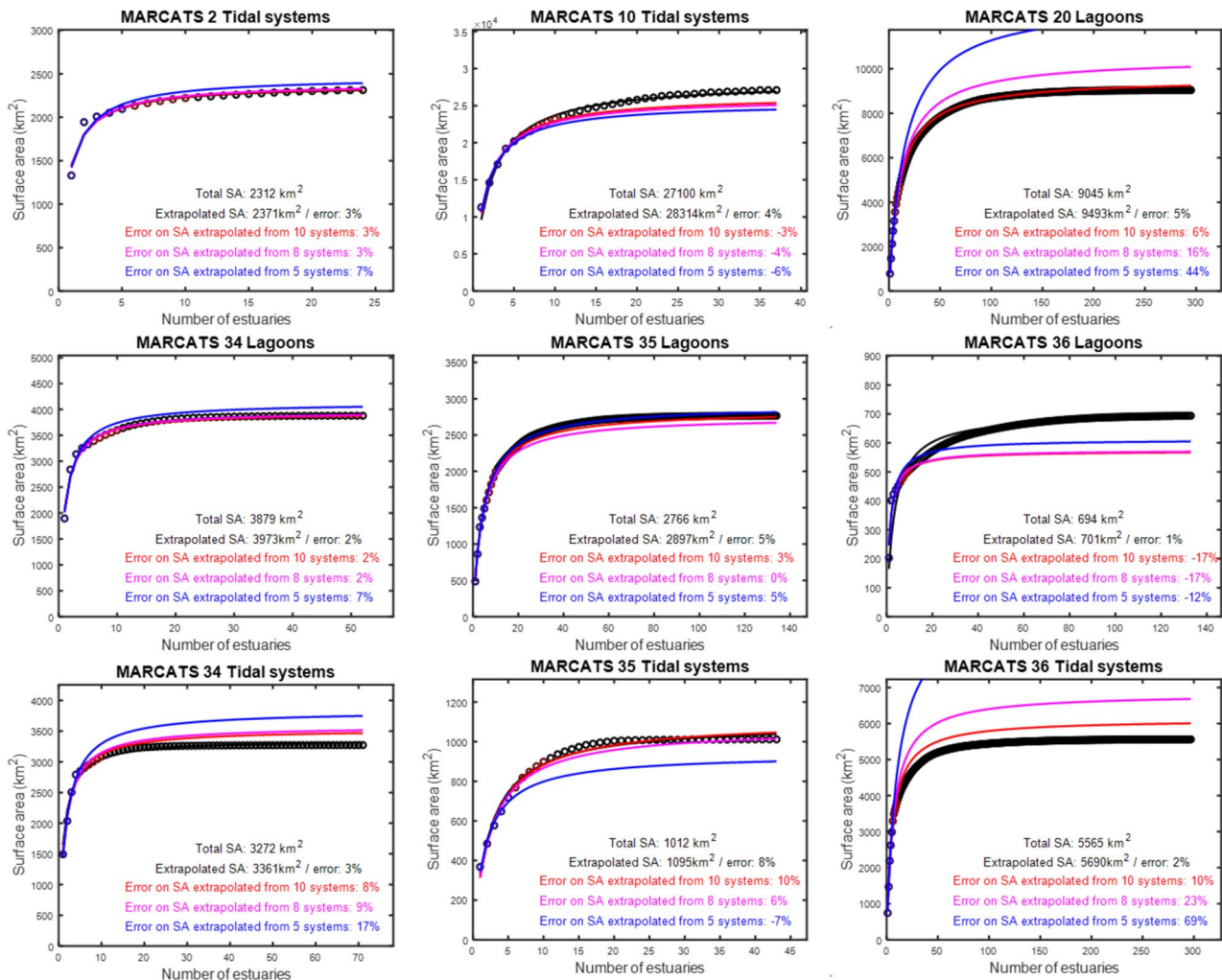


Fig. 2 Evaluation of the term δ_M representing the uncertainty over our interpolation method for 9 MARCATS for which the total surface area is known through the application of our extrapolation method using the 5, 8, or 10 largest estuaries of the region only

then used as the best estimate for δ_M , Δ_M being simply the product of the appropriate δ_M (depending on the number of systems used to perform the extrapolation) and the corresponding surface area.

Because uncertainties of estuarine surface areas have only seldom been reported in previous studies, providing a value for δ_{Si} is somewhat speculative. This uncertainty encompasses several sources of potential errors ranging from the technical limitations associated with the spatial resolution of the map or dataset itself to the determination of the boundaries of the system or the use of inconsistent definitions of estuarine limits over several systems. To constrain these multiple sources of potential uncertainties, type-specific values of δ_{Si} were obtained by assembling a database of well-studied estuaries for which the surface area had been calculated independently at least three times (including this study, Table 1). For each estuary, the multiple surface area estimates were first normalized to the mean surface area for that given system. All normalized values extracted from our literature search were then aggregated by type (56 for tidal systems and deltas, 45 for lagoons, and 11 for fjords) in order to analyze their distribution (Fig. 3). All resulting distributions were exactly centred around 1 (per design) and successfully tested for normality using a Kolmogorov and Smirnov test with a 95% significance threshold (Massey 1951), except for fjords because of the very limited sample size ($n = 11$). The standard deviations were then calculated and yielded the following type-specific values for δ_{Si} : 15% for tidal systems and deltas, 8% for lagoons, and 4% for fjords.

In order to propagate the uncertainties attributed to the surface areas of each individual system belonging to the same MARCATS, Monte Carlo simulations were performed where the surface area of each system used to perform the spatial extrapolation was randomly recalculated assuming a normal distribution centred on the observed surface area and characterized by δ_{Si} as standard deviation. Attention was paid to re-sort the estuaries by decreasing the surface area in case the random recalculation of the individual surface areas modified the original order. Each Monte Carlo simulation was performed using 200 iterations, which proved sufficient to converge to a consistent mean regional surface area estimate within < 1% (test performed using 100 sets of Monte Carlo simulations for several regions). The mean regional surface area calculated by the Monte Carlo simulation was considered the reference value for subsequent calculations, and the standard deviation around this value was used as Δ_s for the calculation of the total uncertainty.

Using the mean surface area generated by the Monte Carlo simulations, the total uncertainty (Δ_T) for a given estuarine type in a given MARCATS region is obtained using the following formula, in which SA is the total extrapolated estuarine surface area (km²):

$$\Delta_T = \sqrt{\Delta_M^2 + \Delta_S^2} = \sqrt{(SA \times \delta_M)^2 + (\Delta_S)^2} \quad (3)$$

A different strategy had to be used for the few regions and estuary types for which exhaustive surveys were available in the literature, circumventing the need to apply our extrapolation method. This was the case for the lagoons bordering the northern and southern coasts of the Mediterranean Sea (MARCATS 20, Cataudella et al., 2015), and all estuary types located in New Zealand (MARCATS 36) and Australia (MARCATS 33, 34, 35). None of the corresponding databases provided an estimate of the surface area uncertainty, whether for individual systems or cumulated over the entire region. Therefore, the overall uncertainty for these regions was estimated by assuming that the uncertainties corresponding to each system can be approximated by δ_{Si} and propagated quadratically to the entire region using the following formula:

$$\Delta_T = \Delta_S = SA \frac{\delta_{Si}}{\sqrt{n}} \quad (4)$$

where n is the number of systems of a given type within the region, δ_{Si} is the type-specific uncertainty for the considered system, and SA is the total surface area of the n estuaries located in the region. This implies that the calculated relative uncertainty will decrease as the number of involved systems increases and that the total uncertainties in these regions are significantly lower than in other regions considering that there is no uncertainty attributed to the extrapolation.

Regional Aggregation

MARCATS Segmentation

The MARCATS segmentation was designed by Laruelle et al. (2013) to provide a multi-layer global segmentation relevant to both oceanic and terrestrial analysis and upscaling strategies. This approach was designed to build upon the COSCAT segmentation (for COastal Segmentation and related CATCHments, Meybeck et al., 2005), which is a global segmentation of terrestrial land masses aggregating river catchments into relatively homogeneous terrestrial units in terms of climate and hydrology. The MARCATS segmentation defines larger units also accounting for oceanic features such as large-scale coastal currents following the classification of continental shelf seas published by Liu et al. (2010). This simultaneous consideration of oceanic and terrestrial constrains on segmentation units that do not compromise the integrity of river catchments makes the MARCATS segmentation ideally suited for the study of the LOAC (Regnier et al., 2013, 2022). Designed like a set of Matryoshka

Table 1 List of estuarine systems for which several independent surface area estimates have been published (or calculated in the context of this study). Tidal refers to ‘tidal systems and deltas’ and systems identified with * correspond to systems which surface area has been calculated in the context of this study

System	Type	km ²	Reference	km ²	Reference	km ²	Reference
Bay of Brest*	Tidal	135	Laruelle et al. 2009a, b	180	Chauvaud et al. 2000	161	This study
Chesapeake Bay	Tidal	10,073 10,421	Dürr et al. 2011 Alder 2003	11,542	Nixon et al. 1996	11,300	US Database
Delaware Bay	Tidal	1980 1957	Dürr et al. 2011 Alder 2003	1989	Nixon et al. 1996	2700	US Database
Dvina*	Tidal	288	Dürr et al. 2011	321	Alder 2003	358	This study
Gambia*	Tidal	611	Dürr et al. 2011	1167	Alder 2003	831	This study
Gironde	Tidal	604 650	Dürr et al. 2011 Coynel et al. 2016	635 477	Audry et al., 2007 Alder 2003	781	Wei et al. 2022
Guadalquivir	Tidal	38	Dürr et al. 2011	48	Alder 2003	39	de la Paz, 2007
Humber	Tidal	291 156	Dürr et al. 2011 Alder 2003	303	Nedwell et al. 2002	220	Volta et al. 2016a
Loire	Tidal	111 220	Dürr et al. 2011 Coynel et al. 2016	151	Alder 2003	185	Wei et al. 2022
Mahi*	Tidal	245	Dürr et al. 2011	258	Alder 2003	316	This study
Mezen	Tidal	174	Dürr et al. 2011	157	Alder 2003	162	Rimsky-Korsakov et al., 2018
Pearl River*	Tidal	2753 2196	Dürr et al. 2011 Alder 2003	1993	This study	1970	Wong and Cheung 2000
Scheldt	Tidal	383 337	Dürr et al. 2011 Alder 2003	277	Nixon et al. 1996	220	Volta et al. 2016a
Seine	Tidal	143	Dürr et al. 2011	146	Laruelle et al. 2019	103	Alder 2003
St Lawrence	Tidal	12,245	Dürr et al. 2011	12,820	Dinauer 2017	12,781	Dinauer and Mucci 2017
Yangtze*	Tidal	2432	Dürr et al. 2011	3841	Alder 2003	3011	This study
Apalachicola Bay	Lagoon	813	Dürr et al. 2011	554	USGS, 2022	593	US database
Chelem Lagoon	Lagoon	13	Alder 2003	14	Chuang et al. 2017	14	CDELM 2003
Choctawhatchee Bay	Lagoon	246 334	Dürr et al. 2011 USEPA 1999	344	Alder 2003	340	US database
Curonian Lagoon	Lagoon	1602	Dürr et al. 2011	1587	Alder 2003	1584	Stankevicius, 1995
Ebrie Lagoon	Lagoon	596 560	Alder 2003 UNESCO, 2009	536	Pagano et al. 2004	566	Guiral and Ferhi 1992
Galveston Bay	Lagoon	1450	Alder 2003	1460	US database	1550	McCarthy et al., 2018
Laguna de Terminos	Lagoon	1660 1700	Dürr et al. 2011 Salles et al., 2002	1658	Alder 2003	1960	CDELM, 2003
Maracaibo Lake*	Lagoon	12,695	Dürr et al. 2011	13,210	Laval et al. 2005	12,882	This study
Mobile Bay	Lagoon	989 1080	Dürr et al. 2011 US database	1064 958	Alder 2003 Dinnel et al. 1990	1059	McCarthy et al., 2018
Oder Lagoon	Lagoon	844	Dürr et al. 2011	1000	Grelowski et al. 2000	968	This study
Patos Lagoon	Lagoon	9851 10,200	Dürr et al. 2011 Alder 2003	10,000	Castelao and Moller, 2006	9100	This study
Venice Lagoon	Lagoon	388	Dürr et al. 2011	500	Solidoro et al. 2005	432	Sfriso et al. 2019
Vistula Lagoon	Lagoon	740	Dürr et al. 2011	838	This study	838	Chubarenko and Margoński 2008
Baker's fjord	Fjord	1170	Dürr et al. 2011	1300	Alder 2003		
Lake Melville	Fjord	2984 2942	Alder 2003 This study	3069	Herdendorf 1982	3000	Schartup et al. 2015
Sognefjord*	Fjord	898	Dürr et al. 2011	950	Sørnes and Aksnes 2006	955	This study
Trondheims Fjord*	Fjord	1503	Dürr et al. 2011	1372	Alder 2003	1531	Thus study

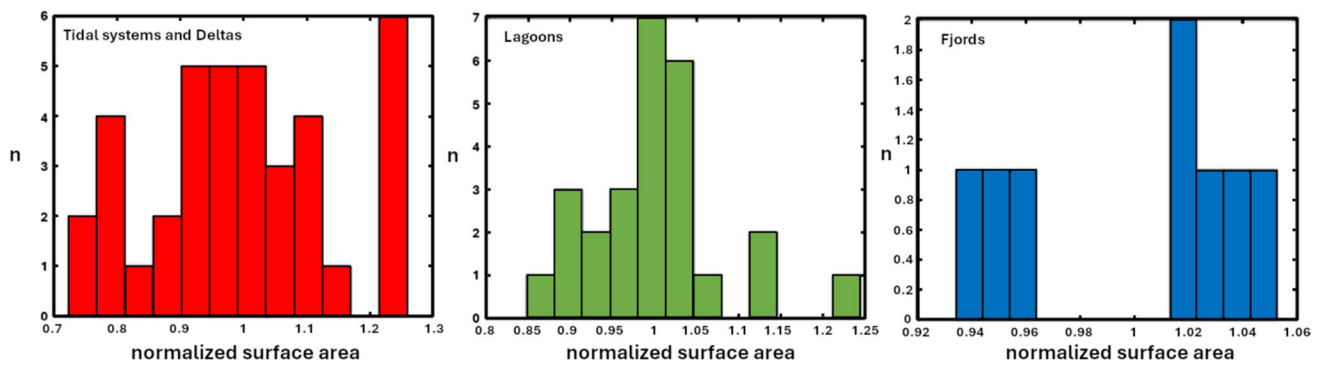


Fig. 3 Histograms of the normalized surface areas of tidal systems and deltas (left), lagoons (middle), and fjords (right)

dolls, the MARCATS segmentation includes 3 nested layers: the river catchment, the COSCAT, and the MARCATS.

The smallest unit of the segmentation is the ~6200 half-degree resolution river catchments defined by a widely used global hydrological network (Seitzinger et al. 2005; Mayorga et al. 2010). At a larger scale, COSCATS segments are groups of these river catchments constrained by similar environmental forcings (e.g. climate, lithology, geology) in which boundaries are defined by geographically explicit features (e.g. mountains, straits). There are 149 exorheic COSCAT units (i.e. regions in which river catchments are ultimately connected to the ocean) in the MARCATS segmentation including 5 for Antarctica, which were not included in Meybeck et al. (2005). Endorheic regions, which are not connected to the ocean, such as the river catchments surrounding the Caspian Sea are thus not included in this segmentation, which primary interest is the connection between land and ocean through the hydrological network. The largest units, MARACTS segments, typically consist in the aggregation of 2 to 6 COSCAT units but some MARCATS (16, 24, 19, 33, 35) only contain a single COSCAT because of very specific coastal features such as a relatively limited upwelling system. MARCATS 20 (the Mediterranean Sea) includes as many as 9 COSCATs. The rationale for the grouping of COSCAT units into a MARCATS was mostly based on the continental shelf classification of Liu et al. (2010) which identified eastern and western boundary currents as well as marginal seas and monsoon-influenced coasts. The remaining continental shelves were distributed among three additional classes based on climatology: polar, sub-polar, and tropical.

RECCAP 2

An important motivation for this regionalized re-evaluation of the global estuarine surface area is to provide a more reliable framework for global GHG budgets such as those previously performed by Borges and Abril (2012), Laruelle et al.

(2010, 2013), and Chen et al. (2013) and now by Rosentreter et al. (2023). Therefore, our results were further aggregated at the continental scale using the global regionalization defined in the context of the RECCAP 2 initiative. Introduced in 2012 during the RECCAP 1 initiative (Canadell et al. 2012), the RECCAP segmentation has been increasingly used since then (e.g. Ciais et al. 2020) including in the recent Global Carbon Project syntheses (Friedlingstein et al. 2022). Several versions of this segmentation have been published since 2012 and the earliest releases used two different sets of regional segmentations for oceans and continents. In the recent RECCAP 2 initiative, however, an effort similar to that of the MARCATS approach was made to design consistent regional limits between both continental land masses and oceans (Ciais et al. 2022). The ten resulting world regions are thus ideally designed to investigate systems such as estuaries, which are located at the interface between continents and oceans (Fig. 4).

In order to provide estuarine surface areas for each RECCAP 2 region, the surface areas of all MARCATS regions entirely included within a RECCAP 2 region were entirely allocated to the latter. For MARCATS where coastlines were distributed over two or more RECCAP 2 regions, the total estuarine surface area was distributed for each type on a pro-rata basis following the surface area-weighted distribution of the ten largest estuarine systems within the MARCATS. For instance, MARCATS 8 (Caribbean Sea) extends through RECCAP 2 regions 1 (North America) and 2 (South America). Six of the ten largest lagoons of MARCATS 8 are located within RECCAP 2 region 1 with a cumulative surface area of 4476 km². This means that 24% of the total surface area of the ten largest lagoons of MARCATS 8 (i.e. 18,505 km²) is located within the geographical boundaries of RECCAP 2 region 1, and, subsequently, 24% of the extrapolated surface area of lagoons for MARCATS 8 (19,692 km²) were allocated to the lagoon surface area of RECCAP 2 region 2. Similar calculations were used for each estuarine type and uncertainties and also propagated in the

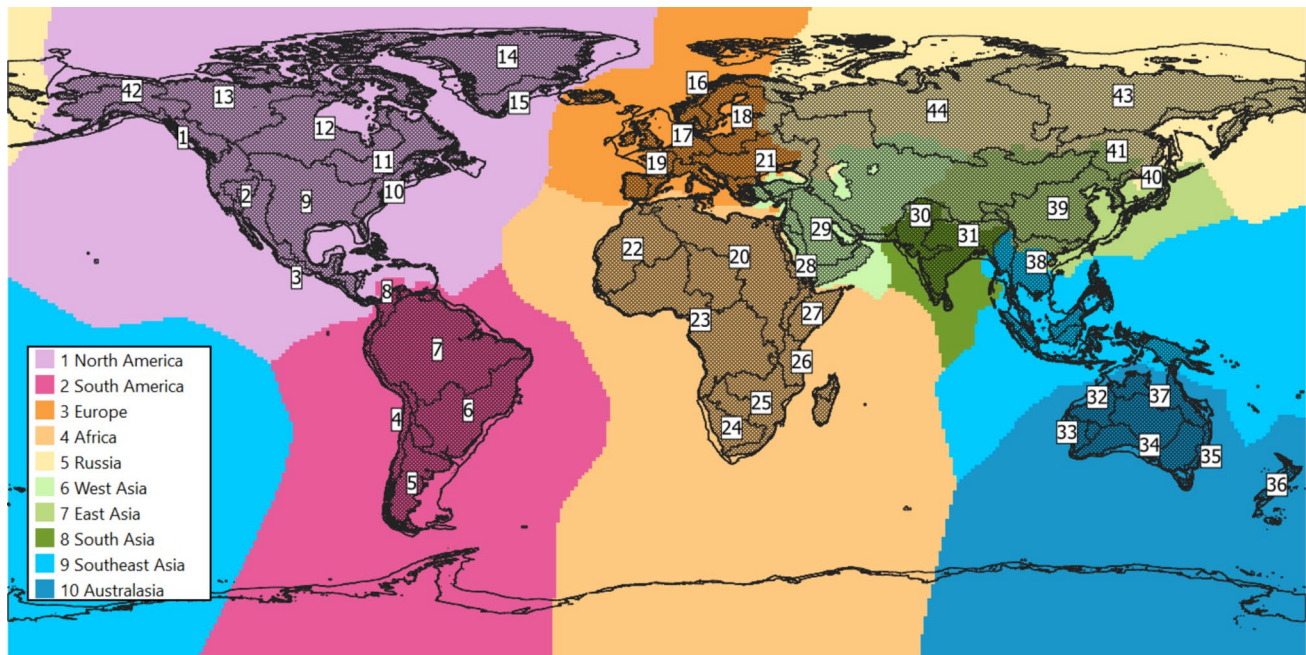


Fig. 4 Delineation of the RECCAP 2 segmentation (in colours) and the MARCATS segmentation (shaded). The geographical extent of the MARCATS segmentation includes all exorheic landmasses and continental shelves until the shelf break as defined in Laruelle et al. (2013)

same fashion using quadratic sums. Using quadratic sums to propagate uncertainties among estuarine types and regions ensures that the global total uncertainties remain consistent when computed by adding the uncertainties of all RECCAP 2 regions or MARCATS.

Other Geometry-Related Calculations

To quantify the potential bias associated with the choice of the upstream boundary of tidal estuaries in the determination of their surface area, we calculated the position of this boundary for a selection of well-known systems using both the end of the tidal influence and the upstream limit of the salinity intrusion as estuarine length. Following the work of Savenije (1986; 2005) which assumes that the geometry of alluvial estuaries can be approximated by an idealized exponential decrease of the estuarine width along its longitudinal axis governed by its so-called convergence length (CL), we used the following equation to determine the width profile of several systems for which sufficient data were available:

$$b_z = b_0 \cdot \exp\left(-\frac{z}{CL}\right) \quad (5)$$

In the equation above, b_z (in m) is the estuarine width at distance z (in km) from the mouth, b_0 is the estuarine width at the mouth (in m), and CL (in km) is the convergence length of the estuary, which characterizes the shape of the system.

Using published data for 19 estuarine systems, for which all parameters required to apply Eq. (5) were available as well as the length of the tidal and saline influences within the estuary, we calculated their respective surface areas using either the end of the tidal influence (LS) or the end of the saline intrusion (LT) as estuarine length. SA_S/SA_T expresses the ratio of the surface area of the ‘saline estuary’ over that of the ‘tidal estuary’ (Table 2).

Finally, the analysis of our results also involved the calculation of linear regressions between our estuarine surface area at the MARCATS scale and the associated length of the coastline, river catchment surface area, and river discharge. These parameters were extracted from the synthesis of Laruelle et al. (2013) for each MARCATS using the global half-degree resolution hydrological network developed by Vörösmarty et al. (2000) in the context of the GlobalNEWS initiative (Seitzinger et al. 2005; Mayorga et al. 2010). The coastline length and river catchment surface areas were extracted using a GIS from the attributes of the shapefile of the GlobalNEWS product while the river discharge corresponded to those calculated for the year 2000 by Fekete et al. (2010). These comparisons were performed to identify potential trends between the geographical parameters and estuarine surface areas to either detect spatial patterns or potentially use these easily accessible parameters as predictors for regional estuarine surface areas.

Table 2 Geometric properties, simulated, and observed salinity intrusion in several tidal estuaries. H , b_0 , CL, LS, LT, and Q represent geometrical and hydrological properties of each system and correspond to the tidal amplitude, the width at the mouth of the estuary, the estuarine convergence length, the length of the salt intrusion, the length of the tidal intrusion, and the riverine freshwater discharge, respectively. SA_S and SA_T correspond to the calculated surface areas of the saline estuary and the surface area of the tidal estuary, respectively. The value SA_S/SA_T reported in the table is thus a unitless number

Estuary	H (m)	b_0 (m)	CL (km)	LS (km)	LT (km)	Q ($\text{m}^3 \text{s}^{-1}$)	SA S/SA T	Reference
Mae Klong	2	250	155	26	120	30	0.29	Savenjie, 2012
Limpopo	1.1	222	18	35	150	10	0.86	Savenjie, 2012
Lalang	2.7	371	96	65	200	50	0.56	Savenjie, 2012
Tha Chin	2.6	3600	87	60	120	5	0.67	Savenjie, 2012
Sinnamary	2.9	2100	39	70	150	10	0.85	Savenjie, 2012
Chao Phya	2.5	500	109	50	120	30	0.55	Savenjie, 2012
Ord	5.9	3200	22.1	50	65	1	0.95	Savenjie, 2012
Incomati	1.4	4500	42	70	100	20	0.89	Savenjie, 2012
Pungue	6.7	6512	21	40	120	10	0.85	Savenjie, 2012
Maputo	3.4	9000	16	90	100	20	0.99	Savenjie, 2012
Thames	4.3	7480	23	50	110	500	0.89	Savenjie, 2012
Corantijn	2.3	30,000	48	16	120	100	0.31	Savenjie, 2012
Gambia	1.2	9687	121	300	500	2	0.93	Savenjie, 2012
Scheldt	3.7	15,207	28	110	200	90	0.98	Savenjie, 2012
Delaware	1.5	37,655	42	140	200	300	0.97	Savenjie, 2012
Seine	4.7	10,000	11	40	168	200	0.97	Laruelle et al. 2019
Loire	4.4	10,000	12	50	114	120	0.98	Wei et al. 2022

Results

Global Distribution

Overall, our calculations yield an updated estimate for the global estuarine surface area of $733,801 \pm 39,892 \text{ km}^2$. Tidal systems and deltas account for $294,956 \pm 30,780 \text{ km}^2$ (~ 40%) while lagoons represent $179,946 \pm 12,056 \text{ km}^2$ (~ 25%) and fjords $259,899 \pm 22,328 \text{ km}^2$ (~ 35%). This updated global estuarine surface area is 27% ($291,777 \text{ km}^2$) lower compared to the most recent estimate of $1,067,198 \text{ km}^2$ (Dürr et al. (2011)). This decrease is particularly pronounced for fjords (43%), followed by lagoons (29%) and tidal systems and deltas (18%) (Table 3). Notably, all global estuary-type specific estimates from Dürr et al. (2011) are well outside the confidence intervals calculated in our study. An estimation of the goodness of fit between the observed cumulative surface areas and those calculated using our extrapolation methods for the largest systems of each MARCATS is calculated using Eq. (2) and reveals a good match between calculated surface areas and observed areas (Fig. 5a). For all estuary-types, the relative errors between observed and calculated surface areas (RRMSE) mostly ranges between 1 and 4%, giving confidence to our extrapolation method. Lagoons showed the largest relative errors with a median error across all MARCATS slightly larger than 3%; however, except for 2 outliers (tidal systems and deltas in MARCATS 12 and lagoons in MARCATS 4), the relative error never exceeds 6% for any estuarine type in any other MARCATS. Also noteworthy is the relative contribution to the total regional surface area of the 10 largest systems within a given MARCATS (Fig. 5b). This

contribution can vary significantly between 60 and 95%, highlighting the disproportionate contribution of the largest estuaries to the total surface area for any given region. This proportion appears to be largest for tidal systems and deltas and smallest for fjords, which could be a reflection of the geomorphologically different origins of these systems. Indeed, beyond the local topography, the shape of deltas and tidal systems is constrained by the dynamic interplay of tidal energy, sediment loads, and riverine discharge (Savenjie 2005; Regnier et al. 2013b), while the shape of fjords is carved into rocks by glaciers over longer timescales (Syvitski, 1987; Bianchi et al. 2020). Our exhaustive survey of individual estuarine surface areas used for our calculations, which includes 735 systems, amounts to cumulated surface areas of $239,005 \text{ km}^2$, $117,195 \text{ km}^2$, and $176,477 \text{ km}^2$, for tidal systems and deltas, lagoons, and fjords, respectively. These surface areas which represent the cumulated surface areas of the 10 largest estuaries of each type in each MARCATS correspond to 81%, 65%, and 68% of the global surface area estimated by our extrapolation method for tidal systems and deltas, lagoons, and fjords, respectively. This implies that a significant fraction of the global estuarine surface area corresponds to the largest systems of a region but also illustrates that uncertainties over our regional estimates are mostly associated with the upscaling of individual estuarine surface area method and its ability to asymptotically approach the parameter a in Eq. (1). Because we performed a thorough literature search to rely as much as possible on already established and published estimates for the surface areas of individual systems in our calculations, two-thirds of these systems correspond to values extracted from previous work. The 277 estuaries that were manually determined

Table 3 Calculated estuarine surface area for each estuary type and MARCATS region. The relative uncertainties reported correspond to 2 σ (95% confidence intervals)

MARCATS region		Tidal systems and deltas	Lagoons	Fjords	Total
Name	Number	km ²	km ²	km ²	km ²
North-eastern Pacific	1	1697 ± 1085	219 ± 124	13,328 ± 2507	15,244 ± 2735
California Current	2	2415 ± 861	6902 ± 1609	0	9317 ± 1825
Tropical Eastern Pacific	3	4365 ± 1610	1879 ± 415	0	6244 ± 1662
Peruvian Upwelling Current	4	85 ± 32	13 ± 7	0	98 ± 32
South America	5	3175 ± 1192	0	21,988 ± 4113	25,163 ± 4282
Brazilian Current	6	21,877 ± 8009	16,346 ± 3807	0	38,223 ± 8868
Tropical Western Atlantic	7	32,809 ± 11,951	0	0	32,809 ± 11,951
Caribbean Sea	8	0	19,692 ± 4309	0	19,692 ± 4309
Gulf of Mexico	9	6213 ± 4723	33,803 ± 8335	0	40,016 ± 9580
Florida Upwelling	10	26,412 ± 10,452	16,086 ± 3874	0	42,498 ± 111,147
Sea of Labrador	11	13,148 ± 14,328	0	11,179 ± 2107	24,327 ± 14,482
Hudson Bay	12	2427 ± 1593	0	10,276 ± 1937	12,703 ± 2508
Canadian Archipelagos	13	6001 ± 3681	3863 ± 921	81,816 ± 15,524	91,680 ± 15,981
Northern Greenland	14	0	0	61,135 ± 13,861	61,135 ± 13,861
Southern Greenland	15	0	0	15,910 ± 3246	15,910 ± 3246
Norwegian Basin	16	0	0	16,534 ± 3141	16,534 ± 3141
North-Eastern Atlantic	17	7721 ± 2985	727 ± 174	5050 ± 942	13,498 ± 3135
Baltic Sea	18	195 ± 121	5567 ± 3120	2722 ± 1467	8484 ± 3450
Iberian Upwelling	19	2805 ± 1073	522 ± 288	0	3327 ± 1111
Mediterranean Sea	20	2051 ± 1292	9787 ± 89	0	11,838 ± 1295
Black Sea	21	4155 ± 1544	2315 ± 536	0	6470 ± 1634
Moroccan Upwelling	22	8779 ± 3785	1223 ± 296	0	10,002 ± 3797
Tropical Eastern Atlantic	23	8911 ± 3355	8812 ± 2152	0	17,723 ± 3986
South-Western Africa	24	208 ± 146	129 ± 73	0	337 ± 163
Agulhas Current	25	1984 ± 1340	1226 ± 298	0	3210 ± 1372
Tropical Western	26	685 ± 422	396 ± 223	0	1081 ± 477
Western Arabian Sea	27	443 ± 282	478 ± 270	0	921 ± 390
Red Sea	28	0	285 ± 68	0	285 ± 68
Persian Gulf	29	1395 ± 639	439 ± 97	0	1834 ± 646
Eastern Arabian Sea	30	5568 ± 2301	2196 ± 1219	0	7764 ± 2604
Bay of Bengal	31	18,907 ± 7931	3101 ± 1711	0	22,008 ± 8113
Tropical Eastern Indian	32	7864 ± 3039	1845 ± 418	0	9709 ± 3067
Leeuwin Current	33	20 ± 2	9773 ± 576	0	9793 ± 576
Southern Australia	34	3272 ± 126	3879 ± 84	0	7151 ± 151
Eastern Australian Current	35	1012 ± 50	2766 ± 37	0	3778 ± 62
New Zealand	36	5564 ± 105	693 ± 9	779 ± 18	7036 ± 106
Northern Australia	37	19,946 ± 8037	1675 ± 384	0	21,621 ± 8046
South East Asia	38	8747 ± 3606	1971 ± 460	0	10,718 ± 3636
China Sea and Kuroshio	39	7189 ± 2537	1513 ± 844	0	8702 ± 2673
Sea of Japan	40	0	696 ± 399	0	696 ± 399
Sea of Okhotsk	41	4268 ± 3068	4592 ± 1100	0	8860 ± 3259
North-western Pacific	42	9020 ± 5789	3966 ± 902	948 ± 509	13,934 ± 5881
Siberian Shelves	43	12,728 ± 4612	8691 ± 1962	0	21,419 ± 5012
Barents and Kara Seas	44	30,895 ± 10,745	1880 ± 443	17,234 ± 3214	50,009 ± 11,224
Global total		294,956 ± 30,780	179,946 ± 12,056	258,899 ± 22,328	733,801 ± 39,892

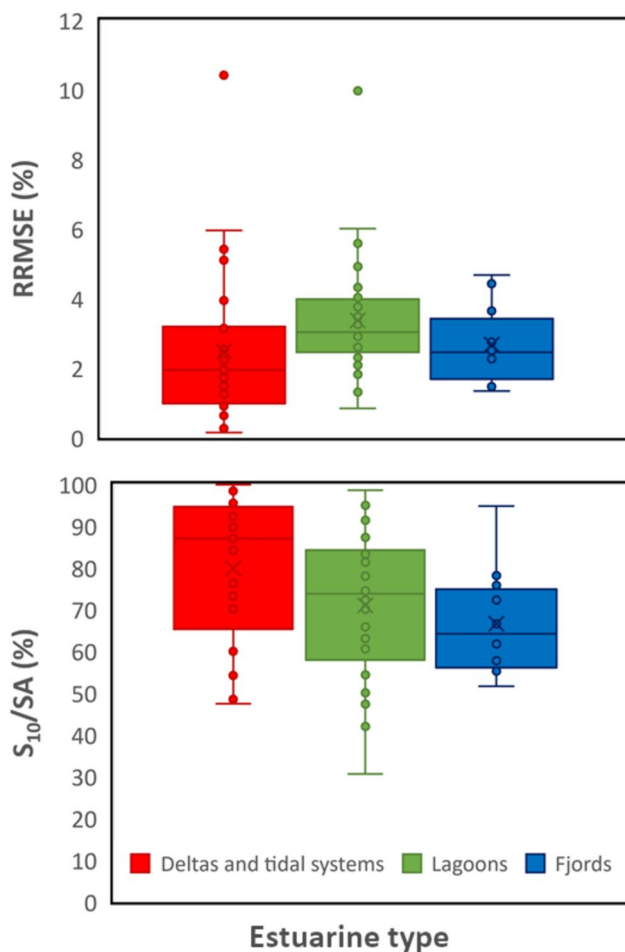


Fig. 5 Distribution of the mean relative error (%) between the fitted and observed estuarine surface areas (RRMSE) within each MARCATS and estuarine type (top) and distribution of the proportion of the total estuarine surface area (SA) represented by the 10 largest systems (S_{10}) within a given MARCATS (bottom)

are located in lesser surveyed regions (i.e. Africa, Southeast Asia, and Russia) and correspond to very small estuaries or coastal features for which we could not find names (such as many fjords surrounding Greenland). Ultimately, only 109 of the systems for which we performed calculations correspond to well-identified estuaries which surface area is larger than 80 km² (Table 4).

The global distribution of estuarine surface areas per MARCATS reveals very pronounced first-order spatial patterns with, naturally, fjords distributed among 13 MARCATS only (Fig. 6a), all located at high latitudes in agreement with Bianchi et al. (2020). It is noteworthy that MARCATS 13, 14, and 15 (i.e. the Canadian Archipelagos and Greenland) account for more than 75% of the global total while the rest of the fjords are distributed among Northern Europe, Russia, New Zealand, and Chile. No clear latitudinal pattern appears to discriminate between the spatial distribution of tidal systems and deltas and of lagoons. However, strong

regional contrasts exist. For instance, tidal systems, deltas, and lagoons located along the Pacific coast of North, Central, and South America, where river catchments are relatively small, gather a cumulated surface area several times smaller than along the Atlantic coast, Arctic regions excluded. Similarly, the Indian Ocean coast of Africa hosts a smaller estuarine surface area than along the Atlantic coast, which is characterized by larger river catchments. We tested the relationship between the surface areas of estuaries and the size of their catchments and found that using linear regression, although statistically significant ($p < 0.05$), the trend at the MARCATS scale was weak ($r^2 = 0.11$) and less significant than the relationships between estuarine surface area and length of the coastline ($r^2 = 0.12$) or between estuarine surface area and river discharge ($r^2 = 0.09$). The regional distribution of surface areas between all three estuarine types is generally consistent with the global estuarine typology of Dürr et al. (2011, Fig. 6b and c). The most notable difference is the larger contribution of lagoons to the estuarine surface areas in Eastern Siberia and along the Pacific coast of China (MARCATS 41 and 43), while these lagoons only represent a relatively small fraction of the coastline. MARCATS where lagoons are largely represented in the typology of Dürr et al. (2011) translate into large surface areas as can be seen around the Gulf of Mexico (MARCATS 9) and the Caribbean Sea (MARCATS 8) or along the Western coast of central Africa (MARCATS 24). Divergences between our calculations and the typology of Dürr et al. (2011) can result from the disproportionate contribution of single large systems (e.g. Lagos lagoon) along the Southern Brazilian coast (MARCATS 5) or in a MARCATS characterized by a relatively small total surface area (MARCATS 33).

RECCAP 2-Scale Aggregation and Comparison with Prior Continental-Scale Estimate

When aggregating the global distribution of estuarine surface areas per estuarine type and RECCAP 2 region, the comparison between the surface areas derived from Dürr et al. (2011) allows us to understand if the downward global revision is homogeneously distributed or if regional patterns emerge (Table 5). Note that the values recalculated after Dürr et al. (2011) for each RECCAP 2 region involve minor rounding discrepancies which lead to a slightly lower total global surface area estimate but the mismatch does not exceed 1%. In both our calculation and that derived from Dürr et al. (2011), North America (RECCAP 2 region 1) contributes the largest share of the global estuarine surface area, with 59% (328,885 km²) and 41% (428.016 km²) in our study and Dürr et al. (2011), respectively. This disproportionate contribution is largely due to Canada's and Greenland's fjords, which account for > 75% of the global surface area of

Table 4 List of significant estuarine systems (> 80 km²) for which a new estimate of the surface area was calculated. Asterisk (*) symbols refers to estuaries already listed in Table 1. Tidal refers to 'tidal systems and deltas'

System	Type	km ²	MARCATS	System	Type	km ²	MARCATS
Amazon	Tidal	14,508	7	Pearl River*	Tidal	1993	38
Tocantin	Tidal	10,223	7	Mekong	Tidal	1277	38
Laguna Bismuna	Lagoon	147	8	Batang Paloh	Tidal	566	38
Maracaibo Lake	Lagoon	12,882	8	Indragiri	Tidal	432	38
Lake Melville*	Fjord	2942	11	Rode river	Tidal	366	38
Nelson Inlet	Tidal	864	12	Musi river	Tidal	340	38
Chesterfield inlet	Fjord	1031	12	Yinyu river	Tidal	304	38
Lyon Inlet	Fjord	984	12	Songkhla Lake	Lagoon	1025	38
Mackenzie river delta	Tidal	5075	13	Dam Thanh Lam	Lagoon	228	38
Bathurst Inlet	Fjord	8506	13	Vinh Cam Ranh	Lagoon	101	38
Sag river	Tidal	212	13	Welu	Lagoon	88	38
Hardangerfjord	Fjord	2426	16	Yangtze*	Tidal	3011	39
Trondheims Fjord*	Fjord	1531	16	Qiantang river	Tidal	982	39
Sognefjord*	Fjord	955	16	Jiaozhou Wan	Tidal	338	39
Rhine river delta	Tidal	910	17	Taedong	Tidal	303	39
Ria de Arosa	Tidal	210	19	Dajing Brook	Tidal	189	39
Bay of Brest*	Tidal	161	19	Minjiang	Tidal	163	39
Ria de Muros e Nioa	Tidal	102	19	Yalu river	Tidal	158	39
Nile River Delta	Tidal	1251	20	Ou river	Tidal	90	39
Rhône River delta	Tidal	319	20	Shancheng gang	Lagoon	99	39
Po River delta	Tidal	95	20	Damenzai	Lagoon	99	39
Ebro River delta	Tidal	94	20	Ogawara KO	Lagoon	88	39
Casamance	Tidal	1222	22	Hamano KO	Lagoon	86	39
Gambia*	Tidal	831	22	Bukhta Ekspeditsii	Lagoon	100	40
Gabon estuary	Tidal	876	23	Nikolaya bay	Lagoon	705	41
Congo	Tidal	700	23	Zaliv Baykal	Lagoon	446	41
Ogooue river	Tidal	444	23	Zaliv Pli'tun	Lagoon	435	41
Rey estuary	Tidal	238	23	Shchastya bay	Lagoon	259	41
Cross estuary	Tidal	237	23	Perevolochnyy Zaliv	Lagoon	250	41
Zambezi	Tidal	234	25	Ozero Tunayacha	Lagoon	175	41
Incomati	Tidal	173	25	Zaliv Nabil'skiy	Lagoon	167	41
Maputo	Tidal	148	25	Zaliv Pomor	Lagoon	153	41
Pungwe	Tidal	140	25	Zaliv Melkovodnyy	Lagoon	133	41
Betsiboka	Tidal	336	26	Anadyr	Tidal	3296	42
Rufiji	Tidal	99	26	Kuskowim river	Tidal	1771	42
Aji river delta	Tidal	394	30	Yukon delta	Tidal	1252	42
Indus river delta	Tidal	343	30	Kvichak	Tidal	149	42
Mahi*	Tidal	316	30	Nushagak River	Tidal	137	42
Ulhas river	Tidal	230	30	Kamtchatka river lagoon	Lagoon	538	42
Sir creek	Tidal	176	30	Mechiginskaya Guba	Lagoon	441	42
Narmada river	Tidal	169	30	Pekul'neyskoye Ozero	Lagoon	440	42
Mid-Ganges	Tidal	6920	31	Avachinskaya Guba	Lagoon	257	42
Eastern-Ganges	Tidal	5868	31	Imuruk Basin	Lagoon	230	42
Hooghly	Tidal	1109	31	Goodnews bay	Lagoon	136	42
Combermere Bay	Tidal	903	31	Lena	Tidal	6340	43
Irrawaddy	Tidal	1570	32	Kolyma	Tidal	1446	43
Salween	Tidal	413	32	Khatanga river	Tidal	1068	43
Pathein river	Tidal	410	32	Yana	Tidal	752	43
Sittaung	Tidal	393	32	Anabar	Tidal	627	43

Table 4 (continued)

System	Type	km ²	MARCATS	System	Type	km ²	MARCATS
Rangoon	Tidal	271	32	Olenyok	Tidal	484	43
Great Tenasserim river	Tidal	226	32	Indigirka	Tidal	311	43
Kra Buri	Tidal	178	32	Khromskaya Bay	Lagoon	1572	43
Dawei river	Tidal	131	32	Omullyakhskaya Guba	Lagoon	918	43
Fly	Tidal	2407	37	Dvina*	Tidal	358	44
Digul River	Tidal	2100	37				

these estuarine systems. Our updated total estuarine surface area for North America is 23% lower compared to Dürr et al. (2011), and the distribution among estuary types also differs with equal contributions of tidal systems and deltas and lagoons in our calculations while the surface area of lagoons is almost twice as large as that of tidal systems and deltas in Dürr et al. (2011). South America (RECCAP 2 region 2) displays the second largest estuarine surface area in our study (111,266 km²) while it is only fourth (79,027 km²) in Dürr et al. (2011). The respective distributions across types are similar in both studies. South America and South Asia (RECCAP 2 region 2 and 8) are the only regions for which our updated surface areas exceed those calculated by Dürr et al. (2011). Europe's (RECCAP 2 region 3) estuarine surface area is less than half our estimation of what was predicted by Dürr et al. (2011) with a significant decrease for tidal systems and deltas as well as for fjords but similar surface areas in lagoons. Africa's (RECCAP 2 region 4) estuarine surface area decreased by a factor of two in our study (37,182 km²) compared to the estimate of 84,733 km² by Dürr et al. (2011). This reduction is mostly attributed to lagoons, which surface area was 46,052 km² in Dürr et al. (2011) and is now only 14,688 km² according to our study. Note that the 10,229 km² of fjords allocated to Africa in Dürr et al. (2011) actually correspond to the Kerguelen Islands which falls within the domain of RECCAP 2 region 4 while being located in the Southern Ocean (see Fig. 4) and is considered devoid of estuaries in our study. Russia (RECCAP 2 region 5) is, after North and South America, the third largest contributor to the global estuarine surface area in our estimate and the second following Dürr et al. (2011). In the latter assessment, fjords dominated the estuarine surface area (33%) in the region while they only contributed 20% in our study. Tidal systems and deltas account for the largest contribution of 58% (48% in Dürr et al. 2011). West Asia's (RECCAP 2 region 6) estuarine surface area mostly corresponds to the coasts surrounding the Arabic peninsula and displays, by far, the smallest estuarine surface area with 2465 km² in our study and 5265 km² in Dürr et al. (2011). In this region, tidal systems and deltas largely dominated the

surface area estimate in Dürr et al. (2011), while in our study, the distribution is almost evenly spread between tidal systems and deltas and lagoons. East Asia (RECCAP 2 region 7) is characterized by the second lowest estuarine surface area in our re-evaluation (12,558 km²), a value that is substantially smaller than the 39,017 km² reported by Dürr et al. (2011) that resulted from a significantly larger contribution of lagoons. South Asia (RECCAP 2 region 8) estuarine surface area is largely dominated by tidal systems and deltas in our study (80%) in contrast to Dürr et al. (2011) that identified lagoons as the highest relative contributor in the region (54%) despite a slightly lower overall surface area in their study (21,585 km²) compared to ours (28,171 km²). Southeast Asia (RECCAP 2 region 9) is the region with the largest discrepancy between both studies: 85,036 km² according to Dürr et al. (2011) and 22,420 km² in our study. This large estimate in Dürr et al. (2011) results from the long coastlines of Indonesia and the Philippines which do not translate into a large estuarine surface area in our approach because of the relatively modest size of the systems found in the region. In both cases, however, these surface areas are largely dominated by tidal systems and deltas (> 80%). Finally, Australasia (RECCAP 2 region 10) shows relatively similar estuarine surface areas in our study (45,880 km²) and in Dürr et al. (2011)'s (51,600 km²) but they are characterized by different distributions among estuarine types which are largely dominated by tidal systems and deltas in Dürr et al. (2011) and more evenly distributed in our study.

Overall, our study thus suggests that the global estuarine surface area is more evenly spread at the continental scale than previously advocated. In spite of yielding a significantly different global estimate for the estuarine surface area, it is worth noting that our work does not contradict the typology of Dürr et al. (2011) in itself with regard to the spatial distribution of estuary types but highlights the limits of using consistent ratios to extrapolate estuarine surface areas from coastlines worldwide. For each estuarine type, the regional surface areas are generally lower with our new calculations but remain within the same order of magnitude (Fig. 7) as those derived from Dürr et al. (2011). Qualitatively, a

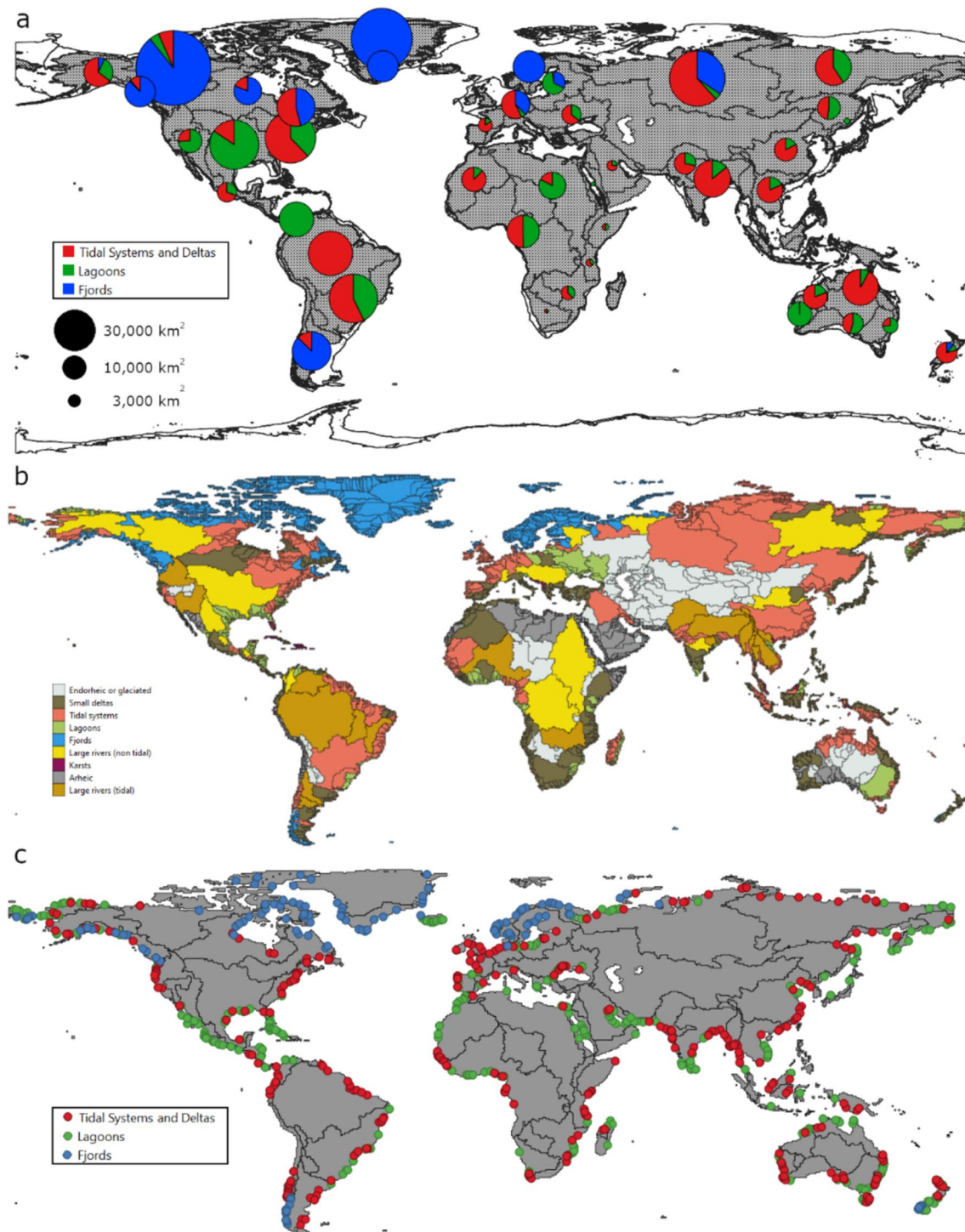


Fig. 6 Estuarine surface areas for each estuary type and MARCATS region shown as pie-charts, where the surface is proportional to the total estuarine surface area of the MARCATS (a); the global estuarine typology of Dürr et al. (2011) (b); and the location of the 737

estuaries used in our calculations (c). For better readability, b the river catchments flowing into each estuary are coloured according to the type of the corresponding estuary

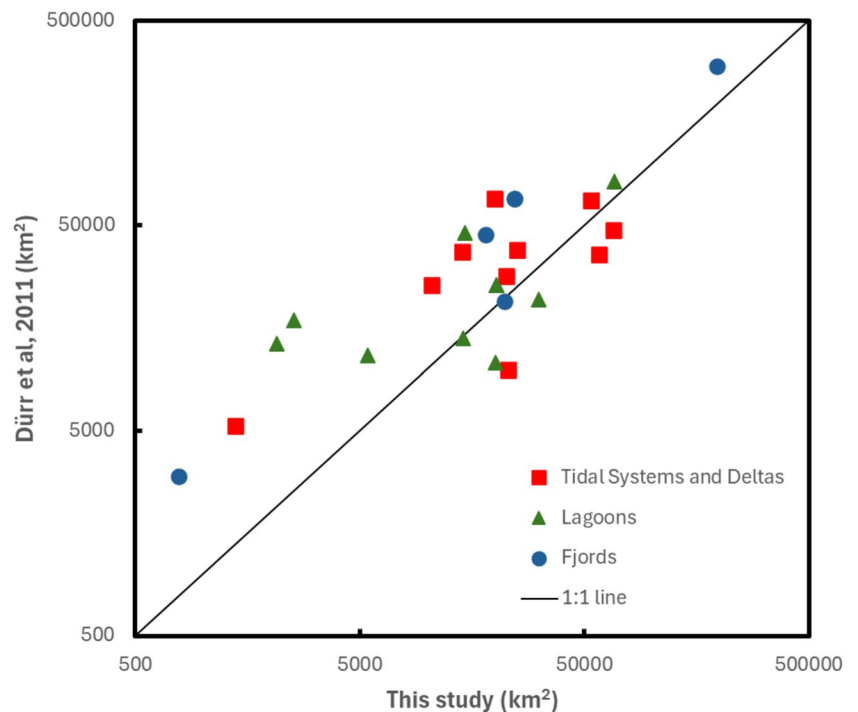
relatively good match can thus be observed between the spatial distributions of the different estuary types in both works. The two studies also make the same assumption that

Antarctica is devoid of estuaries because the vast majority of the Antarctic continent is covered by large ice sheets and does not present persistent aerial rivers able to form

Table 5 Comparison of estuarine surface area for each estuary type and RECCAP2 region according to this study and extrapolated from Dürr et al. (2011). Uncertainties are only available for this study and correspond to 2σ (95% confidence intervals)

RECCAP			Deltas and tidal systems	Lagoons	Fjords	Total
Name	Number	Study	km ²	km ²	km ²	km ²
North America	1	This study	67,197 ± 19,345	68,044 ± 9627	193,644 ± 21,404	328,885 ± 30,415
		Dürr et al. 2011	47,411	82,257	298,348	428,016
South America	2	This study	57,946 ± 14,436	31,332 ± 5349	21,988 ± 4113	111,266 ± 15,935
		Dürr et al. 2011	36,011	21,751	21,265	79,027
Europe	3	This study	14,287 ± 3425	14,452 ± 3154	24,306 ± 3593	53,044 ± 5886
		Dürr et al. 2011	37,270	14,063	67,755	119,088
Africa	4	This study	22,494 ± 5252	14,688 ± 2214	0	37,182 ± 5699
		Dürr et al. 2011	28,452	46,052	10,229	84,733
Russia	5	This study	53,548 ± 12,788	20,200 ± 2483	18,182 ± 3254	91,931 ± 13,427
		Dürr et al. 2011	66,493	25,519	45,265	137,277
West Asia	6	This study	1395 ± 639	1070 ± 178	0	2465 ± 663
		Dürr et al. 2011	5265	0	0	5265
East Asia	7	This study	10,421 ± 3353	2137 ± 924	0	12,558 ± 3478
		Dürr et al. 2011	25,715	13,302	0	39,017
South Asia	8	This study	22,750 ± 7903	5421 ± 1228	0	28,171 ± 7998
		Dürr et al. 2011	9913	11,671	0	21,585
Southeast Asia	9	This study	19,878 ± 6895	2542 ± 236	0	22,420 ± 6899
		Dürr et al. 2011	67,752	17,284	0	85,036
Australasia	10	This study	25,041 ± 6344	20,060 ± 780	779 ± 18	45,880 ± 6392
		Dürr et al. 2011	37,990	10,784	2996	51,770
Global total		This study	294,956 ± 30,780	179,946 ± 12,056	258,899 ± 22,328	733,801 ± 39,892
		Dürr et al. 2011	362,272	242,684	445,859	1,050,815

Fig. 7 Comparison between the regional estuarine surface areas calculated for each RECCAP 2 region and each estuary type by Dürr et al. (2011) and in this study. Note that both axis use logarithmic scales



estuaries when they flow into the coastal ocean. The recent global study on fjords published by Bianchi et al. (2020) and the earlier work from Syvitski (1987) provide a qualitative global distribution of fjords worldwide that is consistent with the global distribution in our study. In their study, Bianchi et al. (2020) only consider a marginal occurrence of fjords in Antarctica at the tip of the Antarctic Peninsula.

Discussion

Revised Global Estuarine Surface Areas

Our updated estimate for the global estuarine surface area of $733,801 \pm 39,892 \text{ km}^2$ presents a significant reduction ($\sim 40\%$) compared to previous assessments (Woodwell et al. 1973; Dürr et al. 2011). This large adjustment reflects the complexity of determining estuarine geomorphology, the lack of global databases, and the relatively limited number of previous regional and global investigations. Perhaps one explanation for the few global assessments of the estuarine surface area was related to the perceived lack of use for such estimations combined with the significant effort required to perform the calculations. The first historical estimate by Woodwell et al. (1973) was in fact not the main purpose of their manuscript, and neither was Dürr et al. (2011)'s. Nevertheless, the citation records of both manuscripts clearly illustrate that their global estuarine surface area estimates have been widely used for upscaling biogeochemical fluxes since the early 2000s (Borges et al., 2004 for CO_2 ; Bange 2006 Barnes and Upstill-Goddard 2011). Such upscaling approaches multiply GHG exchange rate per surface area with the estuarine surface area, either globally (Abril and Borges 2004), per climatic zones (Borges 2005; Borges et al. 2005), regions (Laruelle et al. 2010; Cai 2011; Borges and Abril, 2012), or per estuary type (Laruelle et al. 2013; Chen et al. 2013). At the time of its publication, the estuary-type specific approach by Dürr et al. (2011) not only allowed revisiting (downward) the global estuarine CO_2 budget, but also drew attention to the large contribution of fjords to the total estuarine area, which were typically under-sampled and under-represented in global biogeochemical budgets (Laruelle et al. 2010; Cai 2011; Borges and Abril, 2012; Regnier et al. 2022). The surface area of fjords derived from Dürr et al. (2011) was also later used to constrain the global sequestration of organic carbon in coastal and estuarine sediments (Smith et al. 2015). Moreover, the use of type-specific surface areas in the context of calculating biogeochemical budgets also allowed accounting for the differences in intensity of the biogeochemical processes considered in estuary types (Laruelle et al. 2013). Although performed at a finer spatial scale, our present study follows this tradition

because it was designed in the context of the RECCAP 2 initiative with the aim to update the regional to global GHGs budget for estuaries, published in Rosentreter et al. (2023). More broadly, our past reestimate of the estuarine surface area also fed into the assessment of the role of the Land–Ocean Aquatic Continuum (LOAC) in the global carbon and nitrogen budgets and associated GHGs (Tian et al. 2020; Saunois et al. 2020; Regnier et al., 2103a; Regnier et al. 2022). Furthermore, the present estimate of the regional and global estuarine surface areas was essential and significantly improved the synthesis of Rosentreter et al. (2023), which revealed that estuaries and coastal vegetated ecosystems collectively are greenhouse gas sinks. This assessment was recently integrated into the global N_2O budget (Tian et al. 2024), and it is thus anticipated that our work will be further used in regional and global GHG budget accountings in the near future.

Zooming in on Previously Surveyed Regions

Because estuarine surface areas have rarely been investigated on a large scale, few regional studies can be used to evaluate our updated estimate. Most regional estimates stem from national databases that are already used in our study. However, in the following, we compare our updated estuarine surface areas with previous estimates for the regions of Europe, India, and Mexico.

Europe

The most relevant study our results can be compared to is the evaluation of the surface area of European estuaries by Upstill-Goddard and Barnes (2016). Their estimate of $34,000 \text{ km}^2$ was achieved by extrapolating a ratio of estuarine surface area per coastline length of the UK to the entire European continent. The calculation of such a ratio (but at the global scale) was the core of the approach of Woodwell et al. (1973) and later Dürr et al. (2011) who called this ratio '*w-ratio*' as a reference to Woodwell et al. (1973). Although the details of the calculation were not provided, Upstill-Goddard and Barnes (2016)'s estimate excludes fjords and is thus comparable with our total of $\sim 29,000 \text{ km}^2$ for tidal systems and deltas and lagoons in RECCAP 2 region 3. These similar estimates for Europe contrast with the $\sim 51,000 \text{ km}^2$ suggested by Dürr et al. (2011) and especially the older assessment of $\sim 160,000 \text{ km}^2$ (likely including fjords) reported by Bange (2006). The work by Upstill-Goddard and Barnes (2016) is particularly interesting because, compared to the estimates derived from Dürr et al. (2011) and Bange (2006), it sheds light on how the use of *w-ratios* at global scale can lead to diverging results but can be a more reliable approach regionally, provided that the ratios are calculated on a segment of coast located within the region (Upstill-Goddard and

Barnes 2016). This limitation was also pointed out by Volta et al. (2016a), which found that the cumulative surface area of the estuaries surrounding the North Sea calculated using the *w-ratio* of Dürr et al. (2011) would largely exceed the surface area of all monitored systems in the region. Such regional bias introduced by the use of a globally averaged *w-ratio* that ignores regional geomorphological variability can be overcome by the use of our extrapolation formula, with coefficients fitted independently for each estuarine type in each region using the cumulative surface area of the 10 largest systems of the region.

India

One regional study has provided an estimate of estuarine surface areas (not included in this study) for India and relies on an exhaustive compilation of individual estuarine surface area estimates (Qasim, 2003). The authors estimated the total estuarine surface area of India at 27,000 km². India's coast covers MARCATS 31 and MARCATS 32, with a cumulative estuarine surface area amounting to 31,717 km² (84% for tidal systems and deltas and 16% for lagoons). This number is in reasonable agreement with Qasim (2003)'s estimate considering that MARCATS 32 not only includes the Eastern coast of India but also the coast of Bangladesh which embraces the mega-delta of the Ganges–Brahmaputra rivers. In our study, the latter exceeds 10,000 km², a fraction of which flows into India through the branch of the delta fed by the Hooghly River. The estuarine surface area derived from Dürr et al. (2011) using global *w-ratios* for MARCATS 31 and 32 amounts to 26,300 km², which likely underestimated the actual surface area. This might be attributed to the number of large rivers flowing in the eastern part of India, resulting in more and larger estuaries and deltas over this stretch of coast than the globally averaged *w-ratios* predict.

Mexico

The surface area of all estuaries and lagoons of Mexico has been estimated at 28,500 km² (16,000 for estuaries and 12,500 for lagoons) (Ortiz-Lozano et al. (2005)). In this study, the coast of Mexico is mostly included in MARCATS 2 (on its Atlantic side) and MARCATS 9 (flowing into the Gulf of Mexico) and marginally in MARCATS 8 (Caribbean Sea). The combined surface area of deltas and tidal estuaries of MARCATS 2 and 9 only amounts to 8628 km² while the combined surface area of lagoons of MARCATS 2 and 9 exceeds 40,000 km². However, a significant fraction of these estuaries are located in the United States. Removing this contribution, the remaining total for the two estuary types amounts to ~30,000 km², which is comparable to the Mexico estimate by Ortiz-Lozano et al. (2005), however, with a substantially different distribution between tidal systems

and deltas and lagoons. The surface areas for tidal systems, deltas, and lagoons extracted from Dürr et al. (2011) for MARCATS 2 and 9 are close to the surface areas estimated in our study (40,800 km²) with a similar type distribution. The comparison is difficult to carry further considering that little information is available on the calculations carried out by Ortiz-Lozano et al. (2005) or on their approach how to segregate the two estuary types.

Uncertainties, Limitations, and Future Work

While one of the motivations behind the recent revisions of the global spatial distributions and surface area of inland water and coastal ecosystems often targets the reduction of uncertainty in their geographical extent, surprisingly very few studies have attempted to quantify these uncertainties numerically. This is particularly true for estuaries. To our knowledge, we provide the first global and regional estimation of estuarine surface areas that includes an explicit quantification of uncertainty. This lack of quantitative assessment in previous work can partly be explained by the diversity of potential sources of uncertainties associated with the calculation of the surface area of an estuarine system, let alone the challenge of upscaling such uncertainties at the regional scale. Furthermore, the definition of an estuary and its boundary can significantly vary among authors (Elliott and McLusky, 2002). Consequently, there is no consensus regarding the number of estuaries worldwide. From the lower bound estimate of 4464 proposed by Harris et al. (2016) loosely based on Dürr et al. (2011) to the much larger estimate of 53,000 by McSweeney et al. (2017) derived from GIS calculations using a global digital elevation model, the uncertainty exceeds an order of magnitude. The fact that global high-resolution hydrographical networks such as Hydrosheds (Lehner et al. 2008) connect ~60,000 river catchments to the ocean supports McSweeney et al. (2017)'s estimate but the actual number may be even larger because many small systems may still be missed. Moreover, in large deltaic systems or complex semi-enclosed embayments fed by several rivers, the entire system can either be considered a single estuary or be subdivided into as many estuaries as there are rivers. For instance, the Chesapeake Bay can be considered a single estuary or, based on its numerous feeding rivers, could reach a value as high as several dozen. The choice of one estuary definition over the other will depend on the context and the objectives of a scientific investigation. In global budgeting applications (e.g. Rosentreter et al. 2023), the accuracy of the overall regional surface area is the primary interest and the actual number of estuaries within a given region is less relevant to regional assessments. In the context of a local investigation, however, it may be preferred to define a large system fed by several rivers as several smaller individual estuaries each potentially characterized

by different biogeochemical dynamics controlled by varying discharges and inputs of the rivers (Najjar et al. 2018).

A more quantifiable source of uncertainty relates to the definition of the upstream boundary of an estuarine system. This is illustrated by the calculations performed using idealized estuarine width profiles relying on Savenije (1986; 2005)'s formulation (Eq. 5) on 19 estuarine systems, for which the lengths of the tidal and saline estuaries were available ('Other Geometry-Related Calculations'). While the length of the tidal intrusion generally exceeds that of the saline intrusion by a factor ranging from 1 to 5, the resulting difference in surface area is generally much smaller and below 15% in the majority of the 19 systems investigated (12 systems for which the ratio of the surface areas of the saline estuary over that of the tidal estuary exceeds 0.85, Table 2). Interestingly, the range of surface area differences is comparable to the uncertainty σ_{S_i} of the surface area of individual deltas and tidal systems (see the 'Strategies to Quantitatively Constrain Uncertainties' section).

While our extrapolation strategy is a significant advance from previous estimates (Woodwell et al. 1973; Dürr et al. 2011), the increasing number of recent high-resolution, spatially explicit databases derived from remote sensing imagery and GIS applied in coastal wetlands (Tootchi et al. 2019; Bunting et al. 2022; Murray et al. 2018, 2022) suggests that, ultimately, a similar data product should become available for estuaries. Nevertheless, the complexity of defining estuaries and their boundaries still poses a challenge for large-scale automation based on these technologies. Approaches relying upon remote sensing imagery will have to face additional challenges that have not yet been resolved such as the changing nature of the connection of estuarine systems with adjacent coastal seas which would require a temporal acquisition. Indeed, in their global investigation of Intermittently Closed/Open Lakes and Lagoons (ICOLL), McSweeney et al. (2017) evaluated that ~3% of coastal lagoons worldwide are not permanently connected to the sea throughout the year. It remains an open question how many temporary estuaries exist only after unusual precipitation events in arid regions (Arthington et al. 2014), especially under a future changing climate. As a promising avenue, a tool exploiting readily available spatialized datasets derived from remote sensing has recently been developed (Jiang et al., 2021). This MATLAB algorithm was successfully applied manually to > 100 estuaries surrounding South Korea to calculate the surface area as well as other geometric parameters such as the width at the mouth, the length, and the convergence length of a given estuary. It demonstrates that the algorithm can be applied to a continuous stretch of coast and diagnose a multitude of tidal estuaries, including very small ones. However, this algorithm will likely need

to be modified if deltaic systems with multiple branches or complex lagoon geometries need to be recognized and processed with equal performance. Furthermore, considering the sheer number of estuaries worldwide (conservatively estimated in the tens of thousands by McSweeney et al. 2017), the current lack of an automated procedure remains a major limitation for large-scale applications. Our semi-empirical upscaling method, while still relying on a number of assumptions associated with uncertainties, bridges the gap between a partly outdated estimate (Dürr et al. 2011) and the development of future global remote-sensing-based databases that are still likely several years away.

Conclusions

This study provides a revised global estimate of estuarine surface areas and leads to a significant downward revision compared to the previous assessment by Dürr et al. (2011). Our calculations yield a global estuarine surface area of $733,801 \pm 39,892$ km² (mean $\pm 2 \sigma$), $294,956 \pm 30,780$ km² corresponding to tidal systems and deltas, $179,946 \pm 12,056$ km² corresponding to lagoons, and $259,899 \pm 22,328$ km² corresponding to fjords. Our calculations rely on a new type-specific extrapolation method based on the surface areas of the largest estuaries in each of the 45 MARCATS regions. This approach allows accounting for regional differences in coastal morphologies which were ignored in previous studies that relied on globally averaged estuarine surface area per coastline length. Furthermore, this is the first study that explicitly provides a quantification of uncertainties, which is an important component of regional and global biogeochemical budgets and synthesis efforts (Rosentreter et al., 2023). Our methodology nevertheless remains limited by the complexities in defining estuary boundaries and the inherent uncertainties in upscaling the contribution of small estuarine systems. While our semi-empirical method is a significant advancement, it is still constrained by assumptions and data limitations. The current advances in remote sensing and data processing suggest that these challenges may be overcome in the future but until such tools are available, our updated estimates provide a timely and easy-to-manipulate assessment that can be used in a wide range of large-scale estuarine biogeochemical and ecological applications.

Author Contribution GGL designed the study and performed all the calculations following several discussions with JAR and PR. All authors contributed to the manuscript after an initial draft from GGL.

Funding Goulven G. Laruelle is a research associate of the F.R.S-FNRS at the Université Libre de Bruxelles and acknowledges funding by the nuts-STeauRY project funded by the French

Biodiversity Agency (OFB). Judith A. Rosentreter acknowledges funding by the Yale Institute for Biospheric Studies at Yale University and support by the Australian Research Council through the grants LP190100271, LP200200910, and the Discovery Early Career Award (DE240100305). Pierre Regnier received financial support from the European Union's Horizon 2020 research and innovation programme under grant agreement no. 101003536 (ESM2025—Earth System Models for the Future) and from BELSPO through the project ReCAP, which is part of the Belgian research program FedTwin.

Declarations

Competing Interests The authors declare no competing interests.

Open Access This article is licensed under a Creative Commons Attribution 4.0 International License, which permits use, sharing, adaptation, distribution and reproduction in any medium or format, as long as you give appropriate credit to the original author(s) and the source, provide a link to the Creative Commons licence, and indicate if changes were made. The images or other third party material in this article are included in the article's Creative Commons licence, unless indicated otherwise in a credit line to the material. If material is not included in the article's Creative Commons licence and your intended use is not permitted by statutory regulation or exceeds the permitted use, you will need to obtain permission directly from the copyright holder. To view a copy of this licence, visit <http://creativecommons.org/licenses/by/4.0/>.

References

- Alder, J. 2003. Putting the coast in the Sea Around Us Project. *The Sea around Us Newsletter* 15: 1–2.
- Abril, G., and A. V. Borges. 2004. Carbon dioxide and methane emissions from estuaries. In *Greenhouse gases emissions from natural environments and hydroelectric reservoirs: fluxes and processes*, eds. Tremblay, A., Varfalva, L., C. Roehm, and M. Garneau, 187–207. Springer, Berlin.
- Allen, G. H., and T. M. Pavelsky. 2018. Global extent of rivers and streams. *Science*. <https://doi.org/10.1126/science.aat0636>.
- Arthington, A.H., João Manuel Bernardo, and Maria Ilhéu. 2014. Temporary rivers: linking ecohydrology, ecological quality and reconciliation ecology. *River Research and Applications* 30 (10): 1209–1215. <https://doi.org/10.1002/rra.2831>.
- Audry, S., G. Blanc, J. Schäfer, F. Guérin, M. Masson, and S. Robert. 2007. Budgets of Mn, Cd and Cu in the macrotidal Gironde estuary (SW France). *Marine Chemistry* 107 (4): 433–48.
- Bange, H.W. 2006. Nitrous oxide and methane in European coastal waters. *Estuarine Coastal and Shelf Science*. <https://doi.org/10.1016/j.ecss.2006.05.042>.
- Barbier, E.B., S.D. Hacker, C. Kennedy, E.W. Koch, A.C. Stier, and B.R. Silliman. 2011. The value of estuarine and coastal ecosystem services. *Ecological Monographs*. <https://doi.org/10.1890/10-1510.1>.
- Barnes, J., and R.C. Upstill-Goddard. 2011. N₂O seasonal distributions and air–sea exchange in UK estuaries: Implications for the tropospheric N₂O source from European coastal waters. *Journal of Geophysical Research*. <https://doi.org/10.1029/2009JG001156>.
- Bartley, D. M. 2022. World Aquaculture 2020 – a brief overview, *FAO Fisheries and Aquaculture Circular No. 1233*. Rome, FAO, <https://doi.org/10.4060/cb7669en>
- Battin, T.J., R. Lauerwald, E.S. Bernhardt, E. Bertuzzo, L.G. Gener, R.O. Hall Jr., E.R. Hotchkiss, T. Maavara, T.M. Pavelsky, L. Ran, P. Raymond, J.A. Rosentreter, and P. Regnier. 2023. River ecosystem metabolism and carbon biogeochemistry in a changing world. *Nature* 613: 449–459.
- Bauer, J.E., W.J. Cai, P.A. Raymond, T.S. Bianchi, C.S. Hopkinson, and P.A.G. Regnier. 2013. The changing carbon cycle of the coastal ocean. *Nature*. <https://doi.org/10.1038/nature12857>.
- Bhang, K. J., F. W. Schwartz, H. W. Lee, and S. S. Park. 2019. Scaling effect of lake distribution on power law by coastal area simulation. In *The 3rd international water safety symposium*, eds. Lee, J. L., J.-S. Yoon, W. C. Cho, M. Muin, and J. Lee. *Journal of Coastal Research, Special Issue No. 91*, 301–305. Coconut Creek (Florida), ISSN 0749–0208.
- Bianchi, T.S. 2013. Estuaries: Where the rivers meets the sea. *Nature Education Knowledge* 4 (4): 12.
- Bianchi, T.S., S. Arndt, W.E.N. Austin, D.I. Benn, S. Bertrand, X. Cui, J.C. Faust, K. Kozirowska-Makuch, C.M. Moy, C. Savage, C. Smeaton, R.W. Smith, and J. Syvitski. 2020. Earth-science reviews fjords as aquatic critical zones (ACZs). *Earth-Science Reviews*. <https://doi.org/10.1016/j.earscirev.2020.103145>.
- Billen, G., C. Lancelot, and M. Meybeck. 1991. N, P, and Si retention along the aquatic continuum from land to ocean. In *Ocean margin processes in global change*, ed. R.F.C. Mantoura, J.M. Martin, and R. Wollast, 19–44. New York: John Wiley and Sons.
- Borges, A.V. 2005. Do we have enough pieces of the jigsaw to integrate CO₂ fluxes in the coastal ocean? *Estuaries* 28: 3–27.
- Borges, A. V., and G. Abril, G. 2012. Carbon dioxide and methane dynamics in estuaries. In *Treatise on estuarine and coastal science, Vol. 5*, ed. Wolanski, E., and D. S. McLusky, 119–161, Academic Press.
- Borges, A.V., Delille, B., Schiettecatte, L.S., Gazeau, F., Abril, G., and M. Frankignoulle. 2004. Gas transfer velocities of CO₂ in three European estuaries (Randers FjordScheldt and Thames). *Limnology and Oceanography* 49 (5): 1630–1641. <https://doi.org/10.4319/lo.2004.49.5.1630>.
- Borges, A.V., B. Delille, and M. Frankignoulle. 2005. Budgeting sinks and sources of CO₂ in the coastal ocean: Diversity of ecosystems counts. *Geophysical Research Letters*. <https://doi.org/10.1029/2005GL023053>.
- Bunting, P., A. Rosenqvist, L. Hilarides, R.M. Lucas, N. Thomas, T. Tadono, T.A. Worthington, M. Spalding, N.J. Murray, and L.M. Rebelo. 2022. Global mangrove extent change 1996–2020: Global mangrove watch version 3.0. *Remote Sensing* 14 (15): 3657. <https://doi.org/10.3390/rs14153657>.
- Cai, W.J. 2011. Estuarine and coastal ocean carbon paradox: CO₂ sinks or sites of terrestrial carbon incineration? *Annu. Rev. Marine Sci.* 3: 123–145.
- Canadell, J., P. Ciais, C. Sabine, and F. Joos (Eds.). 2012. Regional Carbon Cycle Assessment and Processes (RECCAP). *Biogeosciences* special issue 107. https://bg.copernicus.org/articles/special_issue107.html.
- Castelão, R.M., and O.O. Möller. 2006. A modeling study of Patos Lagoon (Brazil) flow response to idealized wind and river discharge: Dynamical analysis. *Brazilian Journal of Oceanography* 54 (1): 1–17.
- Cataudella, S., D. Crosetti, and F. Massa. 2015. Mediterranean coastal lagoons: sustainable management and interactions among aquaculture, capture fisheries and the environment studies and reviews. *General Fisheries Commission for the Mediterranean. No 95*, eds Cataudella, S., D. Crosetti, and F. Massa, 278 pp, Rome, FAO
- CDELM (Centro de Documentación “Ecosistemas Litorales Mexicanos”). 2003. Estuarine online database <http://izt.uam.mx/oc/i/index2.html>, last accessed October, 4th 2022.
- Chauvaud, L., F. Jean, O. Ragueneau, and G. Thouzeau. 2000. Long-term variation of the Bay of Brest ecosystem: Benthic-pelagic coupling revisited. *Marine Ecology Progress Series* 200: 35–48

- Chen, C.T.A., and A.V. Borges. 2009. Reconciling opposing views on carbon cycling in the coastal ocean: Continental shelves as sinks and near-shore ecosystems as sources of atmospheric CO₂. *Deep-Sea Res. Pt. II* 56: 578–590.
- Chen, C.T., T.H. Huang, Y.C. Chen, Y. Bai, X. He, and Y. Kang. 2013. Air–sea exchanges of CO₂ in the world’s coastal seas. *Biogeosciences* 10 (10): 6509–6544. <https://doi.org/10.5194/bg-10-6509-2013>.
- Chuang, P.-C., M.B. Young, A.W. Dale, L.G. Miller, J.A. Herrera-Silveira, and A. Paytan. 2017. Methane fluxes from tropical coastal lagoons surrounded by mangroves, Yucatán, Mexico: Methane fluxes from coastal lagoons. *Journal of Geophysical Research. Biogeosciences*. <https://doi.org/10.1002/2017JG003761>.
- Chubarenko, B., and P. Margoński. 2008. The Vistula Lagoon, in: Ecology of Baltic coastal waters. *Ecological studies, vol 197*, eds Schiewer, U., Springer, Berlin, Heidelberg. https://doi.org/10.1007/978-3-540-73524-3_8
- Ciais, P., A. Bastos, F. Chevallier, R. Lauerwald, B. Poulter, J.G. Canadell, G. Hugelius, R.B. Jackson, A. Jain, M. Jones, M. Kondo, I.T. Lujckx, P.K. Patra, W. Peters, J. Pongratz, A.M.R. Petrescu, S. Piao, C. Qiu, C. Von Randow, P. Regnier, M. Saunoy, R. Scholes, A. Shvidenko, H. Tian, H. Yang, X. Wang, and B. Zheng. 2022. Definitions and methods to estimate regional land carbon fluxes for the second phase of the Regional Carbon Cycle Assessment and Processes Project (RECCAP-2). *Geoscientific Model Development* 15: 1289–1316. <https://doi.org/10.5194/gmd-15-1289-2022>.
- Ciais, P., Y. Yao, T. Gasser, A. Baccini, Y. Wang, R. Lauerwald, S. Peng, A. Bastos, W. Li, P.A. Raymond, J.G. Canadell, G.P. Peters, R.J. Andres, J. Chang, C. Yue, A.J. Dolman, V. Haverd, J. Hartmann, G.G. Laruelle, A.G. Konings, A.W. King, Y. Liu, S. Luysaert, F. Maignan, P.K. Patra, A. Pregon, P. Regnier, J. Pongratz, B. Poulter, A. Shvidenko, R. Valentini, R. Wang, G. Broquet, Y. Yin, J. Zscheischler, B. Guenet, D.S. Goll, A.-P. Ballantyne, H. Yang, C. Qiu, and D. Zhu. 2020. Empirical estimates of regional carbon budgets imply reduced global soil heterotrophic respiration. *National Science Review* 8 (2): nwaal45. <https://doi.org/10.1093/nsr/nwaa145>.
- Cloern, J.E., S.Q. Foster, and A.E. Kleckner. 2014. Phytoplankton primary production in the world’s estuarine-coastal ecosystems. *Biogeosciences* 11 (9): 2477–501. <https://doi.org/10.5194/bg-11-2477-2014>.
- Cole, J.J., Y.T. Prairie, N.F. Caraco, W.H. McDowell, L.J. Tranvik, R.G. Striegl, C.M. Duarte, P. Kortelainen, J.A. Downing, J.J. Middelburg, and J. Melack. 2007. Plumbing the global carbon cycle: Integrating inland waters into the terrestrial carbon budget. *Ecosystems* 10: 171–184.
- Coyne, A., L. Gorse, C. Curti, J. Schafer, C. Grosbois, G. Morelli, E. Ducassou, G. Blanc, G.M. Maillat, and M. Mojtabib. 2016. Spatial distribution of trace elements in the surface sediments of a major European estuary (Loire Estuary, France): Source identification and evaluation of anthropogenic contribution. *Journal of Sea Research*. <https://doi.org/10.1016/j.seares.2016.08.005>.
- Crossland, C.J., H.H. Kremer, H.J. Lindeboom, J.I. Marshall Crossland, and M.D.A. LeTissier. 2005. *Coastal fluxes in the Anthropocene, Global Change – The IGBP Series*. Berlin: Heidelberg, Springer.
- Dai, A., and K.E. Trenberth. 2002. Estimates of freshwater discharge from continents: Latitudinal and seasonal variations. *Journal of Hydrometeorology* 3: 660–687.
- DEFRA (Department for Environment, Food and Rural Affairs). 2008. The estuary guide, <http://www.estuary-guide.net/>, Accessed 18 Feb 2009.
- de la Paz, M., Gómez-Parra, A., and J. Forja. 2007. Inorganic carbon dynamic and air–water CO₂ exchange in the Guadalquivir Estuary (SW Iberian Peninsula) *Journal of Marine Systems* 68 (1–2) 265–277. <https://doi.org/10.1016/j.jmarsys.2006.11.011>.
- Digby, M.J., P. Saenger, M.B. Whelan, D. McConchie, B. Eyre, N. Holmes, and D. Bucher. 1998. *A physical classification of Australian estuaries. Report prepared for the urban water research association of Australia by the centre for coastal management*. Lismore: Southern Cross University.
- Dinauer, A. 2017. Inorganic carbon dynamics in the Estuary and Gulf of St. Lawrence: a source or sink of atmospheric carbon dioxide and factors that control the spatial variability in gas exchange. MSc thesis, McGill University (Canada) ProQuest Dissertations Publishing.
- Dinauer, A., and A. Mucci. 2017. Spatial variability in surface-water pCO₂ and gas exchange in the world’s largest semi-enclosed estuarine system: St. Lawrence Estuary (Canada). *Biogeosciences* 14: 3221–3237.
- Dinnel, S.P., W.W. Schroeder, W.J. Jr, and Wiseman. 1990. Estuarine-shelf exchange using Landsat images of discharge plumes. *Journal of Coastal Research* 6 (4): 789–799.
- Downing, J.A., Y.T. Prairie, J.J. Cole, C.M. Duarte, L.J. Tranvik, R.G. Striegl, W.H. McDowell, P. Kortelainen, N.F. Caraco, J.M. Melack, and J.J. Middelburg. 2006. The global abundance and size distribution of lakes, ponds, and impoundments. *Limnology and Oceanography* 51 (5): 2388–97. <https://doi.org/10.4319/lo.2006.51.5.2388>.
- Du, J., and J. Shen. 2016. Water residence time in Chesapeake Bay for 1980–2012. *Journal of Marine Systems* 164: 101–111.
- Dürr, H.H., G.G. Laruelle, C.M. van Kempen, C.P. Slomp, M. Meybeck, and H. Middelkoop. 2011. Worldwide typology of nearshore coastal systems: defining the estuarine filter of river inputs to the oceans. *Estuaries and Coasts* 34: 441–58. <https://doi.org/10.1007/s12237-011-9381-y>.
- Elliott, M., and D.S. McLusky. 2002. The need for definitions in understanding estuaries. *Estuarine, Coastal and Shelf Science* 55: 815–827.
- Elliott, M., A. Whitfield, C. Simenstad, and T. Yanagi. 2024. Introduction to classification of estuarine and nearshore coastal ecosystems. *Treatise on Estuarine and Coastal Science (second Edition)* 1: 1–11. <https://doi.org/10.1016/b978-0-323-90798-9.00127-x>.
- Engle, V.D., J.C. Kurtz, L.M. Smith, C. Chancy, and P. Bourgeois. 2007. A classification of U.S. estuaries based on physical and hydrologic attributes. *Environmental Monitoring and Assessment* 129: 397–412.
- Ericson, J.P., C.J. Vorosmarty, S.L. Dingman, L.G. Ward, and M. Meybeck. 2005. Effective sea-level rise and deltas: Causes of change and human dimension implications. *Global Planetary Change* 50: 63–82.
- Eyre, B. 1998. Transport, retention and transformation of material in Australian estuaries. *Estuaries* 21: 540–551. <https://doi.org/10.2307/1353293>.
- Fekete, B.M., D. Wisser, C. Kroeze, E. Mayorga, L. Bouwman, W.M. Wollheim, and C. Vörösmarty. 2010. Millennium Ecosystem Assessment scenario drivers (1970–2050): Climate and hydrological alterations. *Global Biogeochemical Cycles*. <https://doi.org/10.1029/2009GB003593>.
- Frankignoulle, M., Abril, G., Borges, A., Bourge, I., Canon, C., Delille, B., Libert, E., and J.M. Théate. 1998. Carbon Dioxide Emission from European Estuaries *Science* 282 (5388): 434–436. <https://doi.org/10.1126/science.282.5388.434>.
- Friedlingstein, P., M. O’Sullivan, M. W. Jones, R. M. Andrew, L. Gregor, J. Hauck, C. Le Quéré, I. T. Lujckx, A. Olsen, G. P. Peters, W. Peters, J. Pongratz, C. Schwingshackl, S. Sitch, J. G. Canadell, P. Ciais, R. Jackson, S. R. Alin, R. Alkama, A. Arneth, V. K. Arora, N. R. Bates, M. Becker, N. Bellouin, H. C. Bittig, L. Bopp, F. Chevallier, L. P. Chini, M. Cronin, W. Evans, S. Falk, R. A. Feely, T. Gasser, M. Gehlen, T. Gkritzalis, L. Gloege, G. Grassi, N. Gruber, Ö. Gürses, I. Harris, M. Hefner, R. A.

- Houghton, G. C. Hurtt, Y. Iida, T. Ilyina, A. K. Jain, A. Jersild, K. Kadono, E. Kato, D. Kennedy, K. Klein Goldewijk, J. Knauer, J. I. Korsbakken, P. Landschützer, N. Lefèvre, K. Lindsay, J. Liu, Z. Liu, G. Marland, N. Mayot, M. J. McGrath, N. Metz, N. M. Monacci, D. R. Munro, S.-I. Nakaoka, Y. Niwa, K. O'Brien, T. Ono, P. I. Palmer, N. Pan, D. Pierrot, K. Pockock, B. Poulter, L. Resplandy, E. Robertson, C. Rödenbeck, C. Rodriguez, T. M. Rosan, J. Schwinger, R. Séférian, J. D. Shutler, I. Skjelvan, T. Steinhoff, Q. Sun, A. J. Sutton, C. Sweeney, S. Takao, T. Tanhua, P. P. Tans, X. Tian, H. Tian, B. Tilbrook, H. Tsujino, F. Tubiello, G. R. van der Werf, A. P. Walker, R. Wanninkhof, C. Whitehead, A. Willstrand Wranne, R. Wright, W. Yuan, C. Yue, X. Yue, S. Zaehle, J. Zeng, and B. Zheng. 2022. Global carbon budget 2022. *Earth System Science Data*. <https://doi.org/10.5194/essd-14-4811-2022>.
- Gattuso, J.-P., M. Frankignoulle, and R. Wollast. 1998. Carbon and carbonate metabolism in coastal aquatic ecosystems. *Annual Review of Ecology and Systematics* 29: 405–433.
- Grelowski, A., M. Pastuszek, S. Sitek, and Z. Witek. 2000. Budget calculations of nitrogen, phosphorus and BOD passing through the Oder estuary. *Journal of Marine Systems*. [https://doi.org/10.1016/S0924-7963\(00\)00017-8](https://doi.org/10.1016/S0924-7963(00)00017-8).
- Guiral, D., and A. Ferhi. 1992. Hydrodynamics of Ebrié Lagoon as revealed by a chemical and isotopic study. *Hydrobiologia*. <https://doi.org/10.1007/BF00764766>.
- Harris, P., J. Muelbert, P. Muniz, K. Yin, K. Ahmed, F. Folorunsho, M. Caso, C. C. Vale, J. Machiwa, B. Ferreira, P. Bernal, and J. Rice. 2016. Estuaries and deltas. In *United Nations world ocean assessment*, eds. Inniss, L., A. Simcock, A. Y. Ajawin, A. C. Alcalá, P. Bernal, H. P. Calumpang, P. E. Araghi, S. O. Green, K. Kunio, O. K. Kohata, E. Marschoff, G. Martin, B. P. Ferreira, C. Park, R. A. Payet, J. Rice, A. Rosenberg, R. Ruwa, J. T. Tuhumwire, S. V. Gaever, J. Wang, and J. M. Węśławski. Cambridge University Press, Cambridge.
- Herdendorf, C.E. 1982. Large Lakes of the World. *Journal of Great Lakes Research* 8 (3): 379–412.
- Hume, T., P. Gerbeaux, D. Hart, H. Kettles, and D. Neale. 2016. *A classification of New Zealand's coastal hydrosystems*, 120. Hamilton: Ministry of the Environment.
- Jiang, L.Q., W.J. Cai, and Y. Wang. 2008. A comparative study of carbon dioxide degassing in river- and marine-dominated estuaries. *Limnology and Oceanography* 53 (6): 2603–2615. <https://doi.org/10.4319/lo.2008.53.6.2603>.
- Jung, N.W., G.-H. Lee, Y. Jung, S.M. Figueroa, K.D. Lagamayo, T.-C. Jo, and and., 2021. *J. Chang. Morphest: An Automated Toolbox for Measuring Estuarine Planform Geometry from Remotely Sensed Imagery and Its Application to the South Korean Coast*. *Remote Sens*. <https://doi.org/10.3390/rs13020330>.
- Kang, Y., D. Pan, Y. Bai, X. He, X. Chen, and X., C.-T. A. Chen, and D. Wang. 2013. Areas of the global major river plumes. *Acta Oceanologica Sinica*. <https://doi.org/10.1007/s13131-013-0269-5>.
- Kennish, M. 2002. Environmental threats and environmental future of estuaries. *Environmental Conservation*. <https://doi.org/10.1017/S0376892902000061>.
- Laruelle, G.G. 2009. *Quantifying nutrient cycling and retention in coastal waters at the global scale* PhD dissertation. Utrecht: Utrecht University.
- Laruelle, G.G., P. Regnier, O. Ragueneau, M. Kempa, B. Moriceau, S. Ni Longphuir, A. Leynaert, G. Thouzeau, and L. Chauvaud. 2009a. Benthic-pelagic coupling and the seasonal silica cycle in the Bay of Brest (France): New insights from a coupled physical-biological model. *Marine Ecology-Progress Series* 385: 15–32.
- Laruelle, G. G., V. Roubeix, A. Sferratore, B. Brodherr, D. Ciuffa, D. J. Conley, H. H. Dürr, J. Garnier, C. Lancelot, Q. Le Thi Phuong, J.-D. Meunier, M. Meybeck, P. Michalopoulos, B. Moriceau, S. Ni Longphuir, S. Loucaides, L. Pa push, M. Presti, O. Ragueneau, P. A. G. Regnier, L. Saccone, C. P. Slomp, C. Spiteri, and P. Van Cappellen. 2009. Anthropogenic perturbations of the silicon cycle at the global scale: key role of the land-ocean transition. *Global Biogeochemical Cycles*. <https://doi.org/10.1029/2008GB003267>
- Laruelle, G.G., H.H. Dürr, C.P. Slomp, and A.V. Borges. 2010. Evaluation of sinks and sources of CO₂ in the global coastal ocean using a spatially-explicit typology of estuaries and continental shelves. *Geophysical Research Letters*. <https://doi.org/10.1029/2010GL043691>.
- Laruelle, G.G., H.H. Dürr, R. Lauerwald, J. Hartmann, C.P. Slomp, N. Goossens, and P.A. Regnier. 2013. Global multi-scale segmentation of continental and coastal waters from the watersheds to the continental margins. *Hydrology and Earth System Sciences* 17 (5): 2029–51. <https://doi.org/10.5194/hess-17-2029-2013>.
- Laruelle, G.G., N. Goossens, S. Arndt, W.J. Cai, and P. Regnier. 2017. Air–water CO₂ evasion from US East Coast estuaries. *Biogeosciences*. 14 (9): 2441–68. <https://doi.org/10.5194/bg-14-2441-2017>.
- Laruelle, G.G., A. Marescaux, R. Le Gendre, J. Garnier, C. Rabouille, and V. Thieu. 2019. Carbon dynamics along the Seine River network: Insight from a coupled estuarine/river modeling approach. *Frontiers in Marine Science*. <https://doi.org/10.3389/fmars.2019.00216>.
- Laval, B., J.Y. Imberger, and N. Findikakis. 2005. Dynamics of a large tropical lake: Lake Maracaibo. *Aquatic Sciences* 67 (3): 337–349.
- Leal Filho, W., G.J. Nagy, F. Martinho, M. Saroar, M.G. Erache, A.L. Primo, M.A. Pardal, and C. Li. 2022. *Influences of climate change and variability on estuarine ecosystems: An impact study in selected European, South American and Asian countries*: Int. J. Environ. Res. Public Health. <https://doi.org/10.3390/ijerph19101585>.
- Lehner, B., K. Verdin, and A. Jarvis. 2008. New global hydrography derived from spaceborne elevation data. *Eos, Transactions American Geophysical Union* 89 (10): 93–94.
- Liu, K. K., L. Atkinson, R. Quinones, and L. Talae-McManus (Eds.). 2010. Carbon and nutrient fluxes in continental margins. *Global change – The IGBP Series, 3*, Springer-Verlag Berlin Heidelberg.
- Maavara, T., R. Lauerwald, G.G. Laruelle, Z. Akbarzadeh, N. Bouskill, P. Van Cappellen, and P. Regnier. 2019. Nitrous oxide emissions from inland waters: are IPCC estimates too high? *Global Change Biology* 25 (2): 473–88. <https://doi.org/10.1111/gcb.14504>.
- Mackenzie, F. T., L. M. Ver, C. Sabine, M. Lane, and A. Lerman. 1993. C, N, P, S global biogeochemical cycles and modeling of global change. In *Interactions of C, N, P and S biogeochemical cycles and global change*, eds. Wollast, R., F. T. Mackenzie, and L. Chou, 1–62, Springer-Verlag.
- Mackenzie, F.T., L.M. Ver, and A. Lerman. 1998. Coupled biogeochemical cycles of carbon, nitrogen, phosphorus, and sulfur in the land-ocean-atmosphere system. In *Asian change in the context of global change*, ed. J.N. Galloway and J.M. Melillo, 42–100. Cambridge: Cambridge University Press.
- Mackenzie, F. T., E. H. De Carlo, and A. Lerman. 2012. Coupled C, N, P, and O biogeochemical cycling at the land-ocean interface. In *Treatise on estuarine and coastal science*, eds. Middelburg, J. J., and R. Laane, Ch. 5.10, Elsevier.
- McCarthy, M.J., D.B. Otis, P. Mendez-Lazaro, and F.E. Muller-Karger. 2018. Water quality drivers in 11 Gulf of Mexico estuaries. *Remote Sens (Basel)*. <https://doi.org/10.3390/rs10020255>.
- Mantoura, R. E. C., J. M. Martin, and R. Wollast (Eds.). 1991. Ocean margin processes in global change. p 486. John Wiley & Sons Ltd: Chichester.
- Massey, F.J. 1951. The Kolmogorov-Smirnov test for goodness of fit. *Journal of the American Statistical Association* 46 (253): 68–78.
- Mayorga, E., S.P. Seitzinger, J.A. Harrison, E. Dumont, A.H.W. Beusen, A.F. Bouwman, B.M. Fekete, C. Kroeze, and G. Van

- Drecht. 2010. Global nutrient export from watersheds 2 (NEWS 2): Model development and implementation. *Environmental Modelling and Software* 25 (7): 837–853.
- McKee, B.A., R.C. Aller, M.A. Allison, T.S. Bianchi, and G.C. Kineke. 2004. Transport and transformation of dissolved and particulate materials on continental margins influenced by major rivers: Benthic boundary layer and seabed processes. *Continental Shelf Research* 24: 899–926.
- McSweeney, S.L., D.M. Kennedy, I.D. Rutherford, and J.C. Stout. 2017. Intermittently closed/open lakes and lagoons: Their global distribution and boundary conditions. *Geomorphology* 292: 142–152.
- Meybeck, M., H. H. Dürr, and C. J. Vörösmarty. 2006. Global coastal segmentation and its river catchment contributors: a new look at land-ocean linkage. *Global Biogeochemical Cycles*. <https://doi.org/10.1029/2005GB002540>.
- Murray, N.J., S.R. Phinn, M. DeWitt, R. Ferrari, R. Johnston, M.B. Lyons, N. Clinton, D. Thau, and R.A. Fuller. 2018. The global distribution and trajectory of tidal flats. *Nature*. <https://doi.org/10.1038/s41586-018-0805-8>.
- Murray, N.J., T.A. Worthington, P. Bunting, S. Duce, V. Hagger, C.E. Lovelock, R. Lucas, M.I. Saunders, and M. I., M. Sheaves, M. Spalding, N. J. Waltham, and M. B. Lyons. 2022. High-resolution mapping of losses and gains of Earth's tidal wetlands. *Science*. <https://doi.org/10.1126/science.abm9583>.
- Najjar, R.G., M. Herrmann, R. Alexander, E.W. Boyer, D.J. Burdige, D. Butman, W.-J. Cai, E.A. Canuel, R.F. Chen, M.A.M. Friedrichs, R.A. Feagin, P.C. Griffith, A.L. Hinson, J.R. Holmquist, X. Hu, W.M. Kemp, K.D. Kroeger, A. Mannino, S.L. McCallister, W.R. McGillis, M.R. Mulholland, C.H. Pilskaln, J. Salisbury, S.R. Signorini, P. St-Laurent, H. Tian, M. Tzortziou, P. Vlahos, Z.A. Wang, and R.C. Zimmerman. 2018. Carbon budget of tidal wetlands, estuaries, and shelf waters of Eastern North America. *Global Biogeochemical Cycles* 32: 389–416.
- Nedwell, D.B., L.F. Dong, A. Sage, and G.J.C. Underwood. 2002. Variations of the nutrients loads to the mainland UK estuaries: Correlation with catchment areas, urbanisation and coastal eutrophication. *Estuarine, Coastal and Shelf Science* 54: 951–970.
- Nixon, S.W., J.W. Ammerman, L.P. Atkinson, V.M. Berounsky, G. Billen, W.C. Boicourt, W.R. Boynton, T.M. Church, D.M. Ditoro, R. Elmgren, J.H. Garber, A.E. Giblin, R.A. Jahnke, N.J.P. Owens, M.E.Q. Pilson, and S.P. Seitzinger. 1996. The fate of nitrogen and phosphorus at the land–sea margin of the North Atlantic Ocean. *Biogeochemistry* 3: 141–180.
- Ortiz-Lozano, L., A. Granados-Barba, V. Solís-Weiss, and M.A. García-Salgado. 2005. Environmental evaluation and development problems of the Mexican Coastal Zone. *Ocean & Coastal Management*. <https://doi.org/10.1016/j.ocecoaman.2005.03.001>.
- Pagano, M., E. Kouassi, R. Arfi, M. Bouvy, and L. SaintJean. 2004. In situ spawning rate of the Calanoid Copepod *Acartia clausi* in a tropical lagoon (Ebrié, Côte d'Ivoire): Diel variations and effects of environmental factors. *Zoological Studies* 43 (2): 244–254.
- Potter, I.C., B.M. Chuwen, S.D. Hoeksema, and M. Elliott. 2010. The concept of an estuary: A definition that incorporates systems which can become closed to the ocean and hypersaline. *Estuarine, Coastal and Shelf Science* 87: 497–500.
- Pritchard, D. W. 1967. What is an estuary: physical viewpoint. In *Estuaries*, ed. G. H. Lauf, 3–5, Pub 83, American Association for the Advancement of Science (AAAS): Washington DC.
- Qasim, S.Z. 2003. Production in some tropical environments. In *Marine production mechanics*, ed. M.J. Dunbar, 31–70. Cambridge Univ: Press, London.
- Rabouille, C., F.T. Mackenzie, and L.M. Ver. 2001. Influence of the human perturbation on carbon, nitrogen, and oxygen biogeochemical cycles in the global coastal ocean. *Geochim. Cosmochim. Ac.* 65: 3615–3641.
- Regnier, P., A. Mouchet, R. Wollast, and F. Ronday. 1998. A discussion of methods for estimating residual fluxes in strong tidal estuaries. *Continental Shelf Research* 18: 1543–1571.
- Regnier, P., P. Friedlingstein, P. Ciais, F.T. Mackenzie, N. Gruber, I. Janssens, G.G. Laruelle, R. Lauerwald, S. Luysaert, A.J. Andersson, S. Arndt, C. Arnosti, A.V. Borges, A.W. Dale, A. Gallego-Sala, Y. Goddérès, N. Goossens, J. Hartmann, C. Heinze, T. Ilyina, F. Joos, D.E. LaRowe, J. Leifeld, F.J.R. Meysman, G. Munhoven, P.A. Raymond, R. Spahni, P. Suntharalingam, and M. Thullner. 2013a. Anthropogenic perturbation of the land to ocean carbon flux. *Nature Geoscience*. <https://doi.org/10.1038/NNGEO1830>.
- Regnier, P., S. Arndt, N. Goossens, C. Volta, G.G. Laruelle, R. Lauerwald, and J. Hartmann. 2013. Modelling estuarine biogeochemical dynamics: from the local to the global scale. *Aquatic Geochemistry* 19: 591–626. <https://doi.org/10.1007/s10498-013-9218-3>.
- Regnier, P., L. Resplandy, R.G. Najjar, and P. Ciais. 2022. The land-to-ocean loops of the global carbon cycle. *Nature*. <https://doi.org/10.1038/s41586-021-04339-9>.
- Reinhart, V., P. Hoffmann, D. Rechid, J. Böhner, and B. Bechtel. 2022. High-resolution land use and land cover dataset for regional climate modelling: a plant functional type map for Europe 2015. *Earth System Science Data* 14: 1735–1794. <https://doi.org/10.5194/essd-14-1735-2022>.
- Rimskiy-Korsakov, N.A., Korotaev, V.N., Ivanov, V.V., Pronin, A.A., and N.A. Demidenko. 2018. Hydrological Regime and lithodynamic processes in the Mezen river. *Estuary Oceanology* 58 (4): 593–600. <https://doi.org/10.1134/S0001437018040070>.
- Rosentreter, J.A., G.G. Laruelle, H.W. Bange, T.S. Bianchi, J.J.M. Busecke, W.-J. Cai, B.D. Eyre, I. Forbrich, E.Y. Kwon, T. Maavara, N. Moosdorf, R.G. Najjar, V.V.S.S. Sarma, B. Van Dam, and P. Regnier. 2023. Coastal vegetation and estuaries collectively reduce global warming. *Nature Climate Change* 13 (6): 579–87. <https://doi.org/10.1038/s41558-023-01682-9>.
- Sagar, B.S.D. 2007. Universal scaling laws in surface water bodies and their zones of influence. *Water Resources Research*. <https://doi.org/10.1029/2006WR005075>.
- Salles, P., Silva, R., and J.C. Espinal. 2002. *Waves in inlets*. Conference Proceedings of the 11th Conference on Physics of Estuaries and Coastal Seas, Hamburg, Germany.
- Santoro, M., O. Cartus, N. Carvalhais, D.M.A. Rozendaal, V. Avitabile, A. Araza, S. de Bruin, M. Herold, S. Quegan, P. Rodríguez-Veiga, H. Balzter, J. Carreiras, D. Schepaschenko, M. Korets, M. Shimada, T. Itoh, Á. Moreno Martínez, J. Cavlovic, R. Cazzolla Gatti, P. da Conceição Bispo, N. Dewnath, N. Labrière, J. Liang, J. Lindsell, E.T.A. Mitchard, A. Morel, A.M. Pacheco Pascagaza, C.M. Ryan, F. Slik, G. Vaglio Laurin, H. Verbeeck, A. Wijaya, and S. Willcock. 2021. The global forest above-ground biomass pool for 2010 estimated from high-resolution satellite observations. *Earth System Science Data*. 13 (8): 3927–50. <https://doi.org/10.5194/essd-13-3927-2021>.
- Saunio, M., A.R. Stavert, B. Poulter, P. Bousquet, J.G. Canadell, R.B. Jackson, P.A. Raymond, E.J. Dlugokencky, S. Houweling, P.K. Patra, P. Ciais, V.K. Arora, D. Bastviken, P. Bergamaschi, D.R. Blake, G. Brailsford, L. Bruhwiler, K.M. Carlson, M. Carrol, S. Castaldi, N. Chandra, C. Crevoisier, P.M. Crill, K. Covey, C.L. Curry, G. Etiope, C. Frankenberg, N. Gedney, M.I. Hegglin, L. Höglund-Isaksson, G. Hugelius, M. Ishizawa, A. Ito, G. Janssens-Maenhout, K.M. Jensen, F. Joos, T. Kleinen, P.B. Krummel, R.L. Langenfelds, G.G. Laruelle, L. Liu, T. Machida, S. Maksyutov, K.C. McDonald, J. McNorton, P.A. Miller, J.R. Melton,

- I. Morino, J. Müller, F. Murguia-Flores, V. Naik, Y. Niwa, S. Noce, S. O'Doherty, R.J. Parker, C. Peng, S. Peng, G.P. Peters, C. Prigent, R. Prinn, M. Ramonet, P. Regnier, W.J. Riley, J.A. Rosentreter, A. Segers, I.J. Simpson, H. Shi, S.J. Smith, L.P. Steele, B.F. Thornton, H. Tian, Y. Tohjima, F.N. Tubiello, A. Tsuruta, N. Viovy, A. Voulgarakis, T.S. Weber, M. van Weele, G.R. van der Werf, R.F. Weiss, D. Worthy, D. Wunch, Y. Yin, Y. Yoshida, W. Zhang, Z. Zhang, Y. Zhao, B. Zheng, Q. Zhu, Q. Zhu, and Q. Zhuang. 2020. The global methane budget 2000–2017. *Earth System Science Data* 12: 1561–1623. <https://doi.org/10.5194/essd-12-1561-2020>.
- Savenije, H. 2005. *Salinity and tides in alluvial estuaries*. Amsterdam, The Netherlands: Elsevier.
- Savenije, H.H.G. 2005. *Salinity and Tides in Alluvial Estuaries*, 1st Edn. Elsevier, Amsterdam, The Netherlands.
- Savenije, H. H. G. (Ed.) 2012. *Salinity and tides in alluvial estuaries*, 2nd Edn., available at: <https://salinityandtides.com/> (last access: 8 March 2015).
- Savenije, H.H.G. 1986. A one-dimensional model for salinity intrusion in alluvial estuaries. *Journal of Hydrology* 85 (1–2): 87–109. [https://doi.org/10.1016/0022-1694\(86\)90078-8](https://doi.org/10.1016/0022-1694(86)90078-8).
- Sayre, R., S. Noble, S. Hamann, R. Smith, D. Wright, S. Breyer, K. Butler, K. Van Graafeiland, C. Frye, D. Karagulle, D. Hopkins, D. Stephens, K. Kelly, Z. Basher, D. Burton, J. Cress, K. Atkins, D.P. Van Sistine, B. Friesen, R. Allee, T. Allen, P. Aniello, I. Asaad, M.J. Costello, K. Goodin, P. Harris, M. Kavanaugh, H. Lillis, E. Manca, F. Muller-Karger, B. Nyberg, R. Parsons, J. Saarinen, J. Steiner, and A. Reed. 2018. A new 30 meter resolution global shoreline vector and associated global islands database for the development of standardized ecological coastal units. *J. Oper Oceanogr.* <https://doi.org/10.1080/1755876x.2018.1529714>.
- Schartup, A.T., P.H. Balcom, A.L. Soerensen, K.J. Gosnell, R.S.D. Calder, R.P. Mason, and E.M. Sunderland. 2015. Freshwater discharges drive high levels of methylmercury in Arctic marine biota. *PNAS* 112 (38): 11789–11794.
- Seitzinger, S.P., J.A. Harrison, E. Dumont, A.H.W. Beusen, and A.F. Bouwman. 2005. Sources and delivery of carbon, nitrogen, and phosphorus to the coastal zone: An overview of Global Nutrient Export from Watersheds (NEWS) models and their application. *Global Biogeochemical Cycles*. <https://doi.org/10.1029/2005GB002606>.
- Seitzinger, S.P., and C. Kroeze. 1998. Global distribution of nitrous oxide production and N inputs in freshwater and coastal marine ecosystems *Global Biogeochemical Cycles* 12 (1): 93–113. <https://doi.org/10.1029/97GB03657>.
- Sfriso, A., A. Buosi, M. Mistri, C. Munari, P. Franzoi, and A.A. Sfriso. 2019. Long-term changes of the trophic status in transitional ecosystems of the northern Adriatic Sea, key parameters and future expectations: The lagoon of Venice as a study case. *Nature Conservation*. <https://doi.org/10.3897/natureconservation.34.30473>.
- SMHI (Swedish Oceanographic Data Center). 2009. <http://www.smhi.se/cmp/jsp/polopoly.jsp?d=5431&l=sv>, Accessed 1 May 2009.
- Smith, R.W., T.S. Bianchi, M. Allison, C. Savage, and V. Galy. 2015. High rates of organic carbon burial in fjord sediments globally. *Nature Geoscience* 8: 450–453.
- Solidoro, C., R. Pastres, and G. Cossarini. 2005. Nitrogen and plankton dynamics in the lagoon of Venice. *Ecological Modelling*. <https://doi.org/10.1016/j.ecolmodel.2004.11.009>.
- Sørnes, T.A., and D.L. Aksnes. 2006. Concurrent temporal patterns in light absorbance and fish abundance. *Marine Ecology Progress Series* 325: 181–186.
- Stankevicius, A. (ed.). 1995. *Annual report of scientific work*. 1–90, Klaipėda, Center of Marine Research.
- Syvitski, J.P.M., D.C. Burrell, and J.M. Skei. 1987. *Fjords: Processes and products*. New York: Springer.
- Tian, H., R. Xu, J.G. Canadell, R.L. Thompson, W. Winiwarter, P. Suntharalingam, E.A. Davidson, P. Ciais, R.B. Jackson, G. Janssens-Maenhout, M.J. Prather, P. Regnier, N. Pan, S. Pan, G.P. Peters, H. Shi, F.N. Tubiello, S. Zaehle, F. Zhou, A. Arneeth, G. Battaglia, S. Berthet, L. Bopp, A.F. Bouwman, E.T. Buitenhuis, J. Chang, M.P. Chipperfield, S.R.S. Dangal, E. Dlugokencky, J.W. Elkins, B.D. Eyre, B. Fu, B.D. Hall, A. Ito, F. Joos, P.B. Krummel, A. Landolfi, G.G. Laruelle, R. Lauerwald, W. Li, S. Lienert, T. Maavara, M. Macleod, D.B. Millet, S. Olin, P.K. Patra, R.G. Prinn, P.A. Raymond, D.J. Ruiz, G.R. van der Werf, N. Vuichard, J. Wang, R.F. Weiss, K.C. Wells, C. Wilson, J. Yang, and Y. Yao. 2020. A comprehensive quantification of global nitrous oxide sources and sinks. *Nature*. <https://doi.org/10.1038/s41586-020-2780-0>.
- Tian, H., N. Pan, R.L. Thompson, J.G. Canadell, P. Suntharalingam, P. Regnier, E.A. Davidson, M. Prather, P. Ciais, M. Muntean, S. Pan, W. Winiwarter, S. Zaehle, F. Zhou, R.B. Jackson, H.W. Bange, S. Berthet, Z. Bian, D. Bianchi, A.F. Bouwman, E.T. Buitenhuis, G. Dutton, M. Hu, A. Ito, A.K. Jain, A. Jeltsch-Thömmes, F. Joos, S. Kou-Giesbrecht, P.B. Krummel, X. Lan, A. Landolfi, R. Lauerwald, Y. Li, C. Lu, T. Maavara, M. Manizza, D.B. Millet, J. Mühle, P.K. Patra, G.P. Peters, X. Qin, P. Raymond, L. Resplandy, J.A. Rosentreter, H. Shi, Q. Sun, D. Tonina, F.N. Tubiello, G.R. van der Werf, N. Vuichard, J. Wang, K.C. Wells, L.M. Western, C. Wilson, J. Yang, Y. Yao, Y. You, and Q. Zhu. 2024. Global nitrous oxide budget (1980–2020). *Earth Syst. Sci. Data* 16: 2543–2604. <https://doi.org/10.5194/essd-16-2543-2024>.
- Tootchi, A., A. Jost, and A. Ducharme. 2019. Multi-source global wetland maps combining surface water imagery and groundwater constraints. *Earth System Science Data*. 11 (1): 189–220. <https://doi.org/10.5194/essd-11-189-2019>.
- Schwartz, M.L. 2005. *Encyclopedia of coastal science*. Dordrecht: Springer.
- UNESCO-IOC. 2009. African oceans and coasts. In *IOC Information Document, 1255*. eds. Odido, M., and S. Mazzilli, UNESCO Regional Bureau for Science and Technology in Africa, Kenya.
- Upstill-Goddard, R.C., and J. Barnes. 2016. Methane emissions from UK estuaries: re-evaluating the estuarine source of tropospheric methane from Europe. *Marine Chemistry*. 180: 14–23. <https://doi.org/10.1016/j.marchem.2016.01.010>.
- USEPA. 1999. *Ecological condition of estuaries in the Gulf of Mexico, EPA 620-R-98-004*, U.S. Environmental Protection Agency, Office of Research and Development, National Health and Environmental Effects Research Laboratory, Gulf Ecology Division, Gulf Breeze, Florida. 80 pp.
- USGS (United States Geological Survey). 2022. *NAWQA Apalachicola River Basin study*. <http://usgs.gov/nawqa/index.html>, Last access October 5th, 2022.
- Vanderborght, J.P., R. Wollast, M. Loijens, and P. Regnier. 2002. Application of a transport-reaction model to the estimation of biogas fluxes in the Scheldt estuary. *Biogeochemistry*. <https://doi.org/10.1023/A:1015573131561>.
- Van Niekerk, L., J.B. Adams, G.C. Bate, A.T. Forbes, N.T. Forbes, P. Huizinga, S.J. Lamberth, C.F. MacKay, C. Petersen, S. Taljaard, S.P. Weerts, A.K. Whitfield, and T.H. Wooldridge. 2013. Country-wide assessment of estuary health: An approach for integrating pressures and ecosystem response in a data limited environment. *Estuarine, Coastal and Shelf Science* 130: 239–251.
- Ver, L. M. 1998. *Global kinetic models of the coupled C, N, P, and S biogeochemical cycles: implications for global environmental change*. Ph.D. dissertation, University of Hawaii.

- Ver, L.M., F.T. Mackenzie, and A. Lerman. 1999. Biogeochemical responses of the carbon cycle to natural and human perturbations: Past, present, and future. *American Journal of Science* 299: 762–801.
- Volta, C., G.G. Laruelle, and P. Regnier. 2016a. Regional carbon and CO₂ budgets of North Sea tidal estuaries. *Estuarine, Coastal and Shelf Science* 176: 76–90.
- Volta, C., G.G. Laruelle, S. Arndt, and P. Regnier. 2016b. Linking biogeochemistry to hydro-geometrical variability in tidal estuaries: A generic modeling approach. *Hydrology and Earth System Sciences* 20: 991–1030.
- Vörösmarty, C.J., B.M. Fekete, M. Meybeck, and R.B. Lammers. 2000. Global system of rivers: Its role in organizing continental land mass and defining land-to-ocean linkages. *Global Biogeochemical Cycles*. <https://doi.org/10.1029/1999GB900092>.
- Wei, X., J. Garnier, V. Thieu, P. Passy, R. Le Gendre, G. Billen, M. Akopian, and G.G. Laruelle. 2022. Nutrient transport and transformation in macrotidal estuaries of the French Atlantic coast: a modeling approach using the Carbon-Generic Estuarine Model. *Biogeosciences*. 19 (3): 931–55. <https://doi.org/10.5194/bg-19-931-2022>.
- Wells, N.S., D.T. Maher, D.V. Erler, M. Hipsey, J.A. Rosentreter, and B.D. Eyre. 2018. Estuaries as sources and sinks of N₂O across a land use gradient in subtropical Australia. *Global Biogeochemical Cycles*. <https://doi.org/10.1029/2017GB005826>.
- Wong, M. H., and K. C. Cheung. 2000. China estuarine systems: Pearl River Estuary and Mirs Bay. In: *Estuarine systems of the South China Sea region: carbon, nitrogen and phosphorus*. ed. Smith, S.V., V. Dupra, J. I. Marshall Crossland, and C. J. Crossland, LOCIZ Reports and Studies 14, 7–16, LOICZ, Texel, The Netherlands.
- Woodland, R.J., J.R. Thomson, R. Mac Nally, P. Reich, V. Evrard, F.Y. Wary, J.P. Walker, and P.L. Cook. 2015. Nitrogen loads explain primary productivity in estuaries at the ecosystem scale. *Limnology and Oceanography* 60 (5): 1751–62. <https://doi.org/10.1002/lno.10136>.
- Woodwell, G. M., P. H. Rich, and C. A. S. Hall. 1973. Carbon in estuaries. In *Carbon and the biosphere*. eds. Woodwell, G. M., and E. V., 221–240, Pecan, U.S. Atomic Commission, Springfield, VA.

The initial version of this manuscript was published as a preprint on earthArXiv and assigned a doi (<https://doi.org/10.31223/X5X664>). This preprint can be downloaded using the following URL: <https://doi.org/10.31223/X5X664>.